ISSN 1023-9855

胸腔醫學

Thoracic Medicine

The Official Journal of Taiwan Society of Pulmonary and Critical Care Medicine

Vol.33 No.2 April 2018

第三十三卷 第二期

中華民國一〇七年四月

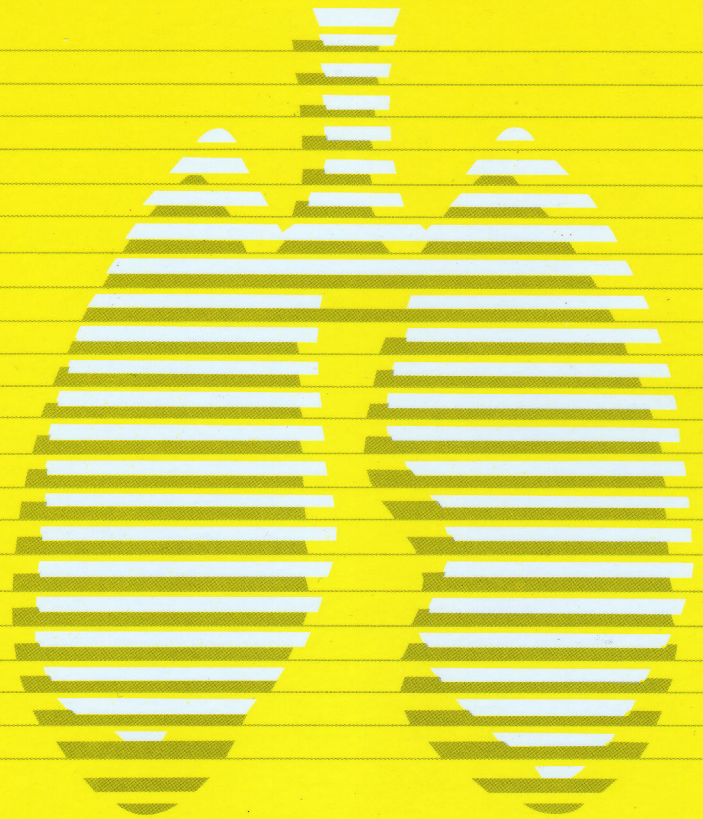

台灣胸腔暨重症加護醫學會

83301 高雄市鳥松區大埤路 123 號

No. 123, Dapi Rd., Niaosong Dist.,
Kaohsiung City 83301, Taiwan

ISSN 1023-9855

中華民國一〇七年四月　第三十三卷　第二期

ISSN 1023－9855

胸腔醫學

Thoracic Medicine

The Official Journal of Taiwan Society of Pulmonary and Critical Care Medicine

Vol.33 No.2 April 2018

原著

病例報告

中華民國一〇七年四月　第三十三卷　第二期

ISSN 1023－9855

胸腔醫學
Thoracic Medicine

The Official Journal of Taiwan Society of Pulmonary and Critical Care Medicine

Vol.33 No.2 April 2018

Orginial Articles

Case Reports

Effects of Angiotensin-Converting Enzyme 2 (ACE2) on Bleomycin-Induced Pulmonary Injury

Wen-Yeh Hsieh*,****, Jih-Sheng Hsieh**, Wan-Hsuan Chuang***,
Chih-Sheng Lin**, Chen-Yi Huang*

Introduction: Anticancer treatment with bleomycin can cause interstitial pneumonitis and pulmonary fibrosis, pathologies that are affected by the renin-angiotensin system (RAS). In this study, we focused on the role of angiotensin-converting enzyme 2 (ACE2), which can hydrolyze angiotensin II (Ang II) to angiotensin-(1-7) (Ang-(1-7)), in bleomycin-induced pulmonary injury.

Methods: Male wild-type (WT; C57BL/6) and ACE2 knockout (KO; hemizygous $ACE2^{-/y}$) mice were anesthetized and given a single dose of bleomycin solution (4 mg/kg) directly into the trachea. The body weight and resting respiratory rate (RRR) of the mice were measured every week, and the mice were sacrificed 3 weeks after bleomycin treatment. Lung tissue was collected for further biochemical and pathological assays.

Results: After bleomycin challenge, the WT and $ACE2^{-/y}$ mice were compared. RRR, infiltration of white blood cells, alveolar damage, fibrosis, and the pulmonary levels of transforming growth factor-β1 (TGF-β1) and interleukin-6 (IL-6) were significantly greater in the $ACE2^{-/y}$ mice than in the WT mice. Pulmonary ACE activity was significantly increased in the $ACE2^{-/y}$ mice and was higher than that in the WT mice. Fibrotic markers, connective tissue growth factor (CTGF) and elastin were markedly induced in the lungs after bleomycin challenge.

Conclusion: Bleomycin can induce sustained pulmonary inflammation, fibrosis, and increased ACE activity. Bleomycin-induced lung injury is related to RAS imbalance, and ACE2 deficiency can enhance this injury via abnormal accumulation of Ang II. The results suggest that regulating the RAS could reduce pulmonary damage caused by bleomycin. ***(Thorac Med 2018; 33: 50-62)***

Key words: bleomycin, pulmonary fibrosis, renin-angiotensin system, angiotensin-converting enzyme 2, inflammation

*Division of Chest Medicine, Department of Internal Medicine, Hsinchu Mackay Memorial Hospital, Hsinchu, Taiwan; **Department of Biological Science and Technology, National Chiao Tung University, Hsinchu, Taiwan; ***Division of Respiratory Therapy, Department of Internal Medicine, Hsinchu Mackay Memorial Hospital, Hsinchu, Taiwan; ****Department of Senior Citizen Service Management, Minghsin University of Science and Technology, Hsinchu, Taiwan

Wen-Yeh Hsieh and Jih-Sheng Hsieh contributed equally to the work for this study as first authors.

Address reprint requests to: Dr. Chen-Yi Huang, Division of Chest Medicine, Department of Internal Medicine, Hsinchu Mackay Memorial Hospital, No. 690, Sec. 2, Guangfu Rd, Hsinchu 300, Taiwan

Introduction

Anticancer treatment with bleomycin can have side effects, such as interstitial pneumonitis and idiopathic pulmonary fibrosis (IPF), in the respiratory system [1]. These side effects are related to the physiological condition of the patients and whether they require cumulative doses of bleomycin. IPF is a progressive, inflammatory, fibrotic, and proliferative lung disease. The disease results in a progressive loss of normal lung structure and gas exchange function [2]. To understand the side effects of fibrosis associated with bleomycin therapy, researchers have attempted to develop murine models of human interstitial pneumonia. Investigations of bleomycin-induced fibrosis in murine models have led to the identification of many pathological cells and mediators that are also believed to be important in human diseases [3-4]. However, the relationship between bleomycin-induced fibrosis and disease pathogenesis is not well understood, and requires more study.

The pathology of IPF is closely related to the regulation of the renin-angiotensin system (RAS), i.e., the angiotensin-converting enzyme (ACE)/angiotensin II (Ang II) axis, in the patient [5-6]. Inhibition of the ACE/Ang II axis has been shown to reduce the pathogenesis of bleomycin-induced fibrosis in murine models [7-8]. However, the role of ACE 2 (ACE2) is not well known. ACE2 is an ACE homologue that hydrolyzes Ang II to angiotensin 1-7 (Ang-(1-7)), a peptide that exerts actions opposite to those of Ang II. In our previous studies, we showed that ACE2 dysregulation is highly associated with fibrotic damage in cardiovascular and pulmonary diseases [9-11]. Potential alternative targets within the RAS are also known to modulate the ACE2/Ang-(1-7)/Mas axis [12]. Montes *et al*. [13] found that lung fibroblasts can produce renin, which is upregulated in IPF. Moreover, studies of severe acute respiratory syndrome (SARS) and acute respiratory distress syndrome (ARDS) revealed that ACE2 could protect against severe acute lung injury in rats [14]. In this study, therefore, we aimed to determine the mechanism of ACE2 regulation of bleomycin-induced pulmonary fibrosis using an experimental mouse model. We focused on exploring the cellular and physiological roles of ACE2 in the pulmonary system and tested the hypothesis that the ACE2/Ang-(1-7) axis has anti-fibrotic effects in this bleomycin-induced pulmonary injury model.

Materials and Methods

Mouse model of lung injury induced by bleomycin treatment

Since *ace2* is an X-linked gene, there are 3 different patterns of DNA genotyping obtained during the breeding of ACE2 KO mice, including heterozygote ($ACE2^{-/+}$; female), homozygote ($ACE2^{-/-}$; female), and hemizygote ($ACE2^{-/y}$; male). Wild-type (WT; C57BL/6) and $ACE2^{-/y}$ male mice at 6 to 8 weeks of age were used in the study. The WT mice were purchased from the National Laboratory Animal Center (NLAC) in Taiwan. The first generation of ACE2 KO (B6; 129S5-Ace2tm1 Lex/Mmcd) mice was obtained from the Mutant Mouse Regional Resource Centers (MMRRC) and was then bred in NLAC [11]. The experimental protocol conformed to the Guide for the Care and Use of Laboratory Animals published by the National Institutes of Health (NIH Publication No. 85-23, revised 1996) and was approved by the animal welfare committees of National Chiao Tung University.

Animal model of lung injury induced by bleomycin treatment

The WT and ACE2 KO ($ACE2^{-/y}$) mice were divided into the following groups: (1) WT control group (Control/PBS; n=5), (2) WT with bleomycin treatment group (WT/BLM; n=5), and (3) $ACE2^{-/y}$ with bleomycin treatment group ($ACE2^{-/y}$/BLM; n=5). The mice were anesthetized using a mixture of 2.5% avertin, and bleomycin was administered intratracheally at a dose of 4 mg/kg in 50 μL. Control animals were intratracheally administrated with 50 μL of sterile PBS. Body weight and resting respiratory rate (RRR) were measured every week. The mice were sacrificed after 3 weeks of bleomycin treatment and then the lungs were isolated for further assay.

RRR Measurement

Mouse RRR (BPM, breaths per minute) was measured as described in our previous study [11]. The RRR was measured using whole body unrestrained chambers (Emka, Middletown, PA, USA) on live mice that were exercised for 10 min at weeks 0, 1, 2, and 3 after bleomycin treatment. Data were collected and analyzed using the BIOPAC student lab systems software package (Biopac system, Goleta, CA, USA).

Protein extraction

The lung samples that were derived from the mice were prepared as previously described [11]. The organ samples were collected and then homogenized 3 to 5 times with PRO-PREPTM Protein Extraction Solution (iNtRON Biotechnology, Kyungki-Do, Korea). Samples were centrifuged at 13,000 xg for 10 min to separate the supernatants and pellets. The total amount of protein in the supernatant was measured using the Bradford dye binding assay (Bio-Rad Laboratories, Hercules, CA, USA), with bovine serum albumin used as the standard. The supernatants were aliquoted and stored at -80°C until further use.

Enzyme-linked immunosorbent assay (ELISA)

Tissue protein was analyzed for transforming growth factor (TGF)-β1 (#E13703-112) and interleukin (IL)-6 (#E09358-1640) using sandwich ELISA kits (eBioscience, San Diego, CA, USA). Tissue protein was incubated in ELISA plates in which the wells had been coated with primary antibodies. Following the addition of biotinylated antibodies, the plates were washed and reacted with horseradish peroxidase (HRP)-conjugated streptavidin. Tetramethylbenzidine (TMB) 1-step substrate was used to detect the targeted protein, and the absorbance at 450 nm was measured using a microplate reader (Thermo Scientific Multiskan EX, Waltham, MA, USA).

Western blotting

Western blot analysis was performed as previously reported [15]. Lung tissue homogenates containing 20 μg of protein were electrophoresed on SDS-PAGE and then transferred onto polyvinylidene fluoride membranes. Primary monoclonal antibodies against elastin (GTX37428; Genetex, Irvine, CA, USA), connective tissue growth factor (CTGF) (GTX 26992; Genetex) and β-actin (AC-15, #A5441; Santa Cruz Biotechnology, Santa Cruz, CA, USA) were used for detection. Protein bands were visualized using enhanced chemiluminescence detection (Immobilon Western Chemiluminescent HRP Substrate; Millipore, Billerica, MA, USA) and by exposing the membranes to Lumi-Film Chemiluminescent Detection Film (Roche, Indianapolis, IN, USA). The bands on

the images were detected at the anticipated location based on size. Band intensity was quantified using Scion Image software (Scion, Frederick, MD, USA). The amounts of elastin and CTGF were expressed relative to the amount of β-actin (as the internal standard) in each sample.

ACE and ACE2 activity assays

ACE and ACE2 activities were assayed using the fluorogenic substrates Mca-YVADAPK and Mca-APK-Dnp (AnaSpec, Fremont, CA, USA), respectively, as reported by Vickers *et al*. [16]. The assay was performed in a quartz microcuvette with 20 μL of lung tissue proteins and 2 μL of the fluorogenic substrate (stock concentrations: 4 mM ACE substrate or 1.5 mM ACE2 substrate) in ACE or ACE2 assay buffer. The reaction was followed kinetically for 1 h using a fluorescence reader at excitation and emission settings of 330 and 390 nm, respectively. All samples were plotted using Grafit v. 4.0 (Sigma-Aldrich, Louis, MO, USA), and enzyme activity was expressed as relative fluorescence units (RFU)/h/ml. To ensure the specificity of the reaction, samples were also assayed independently in the presence of 1 μM captopril (Sigma-Aldrich; a specific ACE inhibitor) or 1 μM DX600 (AnaSpec; a specific ACE2 inhibitor).

Histological determination

Organ samples were isolated from WT and $ACE2^{-/y}$ mice, and a piece of the right lung was excised and fixed in 10% formaldehyde. Mounted sections were prepared and stained with hematoxylin-eosin (H&E) and Masson's trichrome stain. The stained sections were photographed using a digital camera mounted on a microscope. Manual planimetry was performed on the microscope using PALM RoboSoftware v2.2 and H&E-stained sections. A computerized microscope equipped with a high-resolution video camera (BX 51; Olympus, Tokyo, Japan) was used for morphometric analysis. The thickness of airway epithelium was calculated as the difference between the area encompassing the epithelial cell basement membrane and the lumen. This was expressed as the epithelial area.

Statistical analysis

All values are expressed as mean±standard deviation (SD). Student's *t*-test was used for comparisons involving 2 groups, and 1-way analysis of variance (ANOVA) was used to evaluate differences among multiple groups. A value of $P<0.05$ was considered statistically significant.

Results

Bleomycin-induced pulmonary injury in the mice

The WT and $ACE2^{-/y}$ mice were treated with bleomycin (WT/BLM and $ACE2^{-/y}$/BLM group, respectively), and body weight as well as RRR were monitored weekly. After bleomycin treatment for 1 week, the WT/BLM and $ACE2^{-/y}$/BLM mice showed a marked loss of body weight. The initial body weight of these mice was 19.1±0.4 g (WT) and 18.9±0.4 g ($ACE2^{-/y}$). Their weight dropped to 17.4±0.3 g (WT/BLM) and 17.3±0.4 g ($ACE2^{-/y}$/BLM) in the first week after bleomycin challenge ($P<0.01$), but then stabilized to 17.5±0.2 g (WT/BLM) and 17.3±0.3 g ($ACE2^{-/y}$/BLM) 3 weeks after treatment (Figure 1A). In contrast, the control mice (treated with PBS; Control/PBS group) steadily gained weight to 20.2±0.3 g during the experimental period (Figure 1A). The average RRR

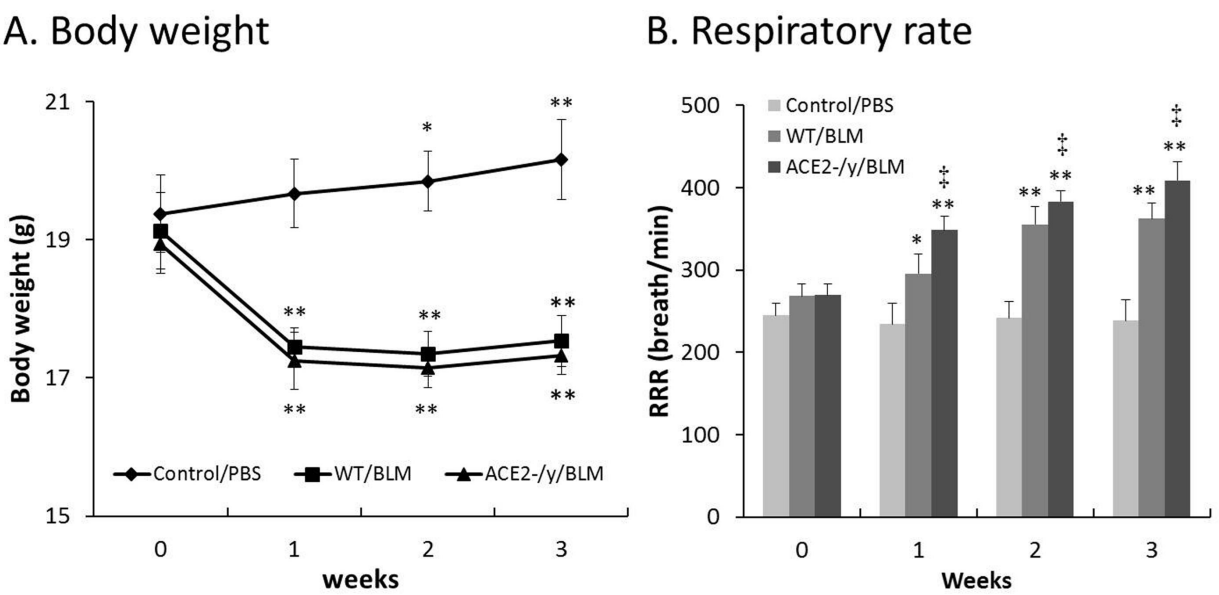

Fig. 1. Physiological Effects of Bleomycin Treatment on Mice. Body weights (A) and resting respiratory rates (RRR) (B) of the WT and ACE2$^{-/y}$ mice (WT/BLM and ACE2$^{-/y}$/BLM groups) treated with bleomycin for 3 weeks were measured weekly. Both the bleomycin-challenged WT and ACE2$^{-/y}$ mice showed reduced body weight and increased RRR relative to their initial values during the first week of bleomycin treatment. All values are expressed as mean±SD of each group; **P*<0.05 and ***P*<0.01 compared with the Control/PBS group, ‡*P*<0.01 compared with the WT/BLM group.

of the WT/BLM and ACE2$^{-/y}$/BLM mice was approximately 260 BPM before the experimental treatment, but the RRR of the mice treated with bleomycin for 3 weeks was significantly increased (P<0.01). The RRR induced by bleomycin treatment was significantly greater in the ACE2$^{-/y}$/BLM mice than in the WT/BLM mice (P<0.01) (Figure 1B). In the WT/BLM mice, the RRR progressively increased to approximately 370 BPM by 3 weeks. By comparison, the RRR of the ACE2$^{-/y}$/BLM mice increased to approximately 400 BPM.

The WT and ACE2$^{-/y}$ mice were treated with bleomycin for 3 weeks, and then the animals were sacrificed to isolate lung tissues for pathological examinations. The lung alveolar and bronchiole sections of the WT/BLM and ACE2$^{-/y}$/BLM mice were stained with H&E, and the results showed that bleomycin treatment promoted white blood cell (WBC) infiltration around the bronchioles (Figure 2A) and damaged alveoli (Figure 2B). The lung tissue sections were also stained with Masson's trichrome for the fibrotic pathology examination. The results showed a significantly increased fibrotic area (stained in blue) in the lungs of the mice with bleomycin treatment (Figure 3). Figures 2 and 3 show that bleomycin treatment may induce more severe histological changes in the lungs of the ACE2$^{-/y}$/BLM mice than those found in the WT/BLM mice.

Pro-inflammatory cytokines in lung injury induced by bleomycin

Through analyzing the expression of cytokines, we were able to confirm that bleomycin treatment could induce pulmonary inflammation in the mice. The levels of pulmonary TGF-β1

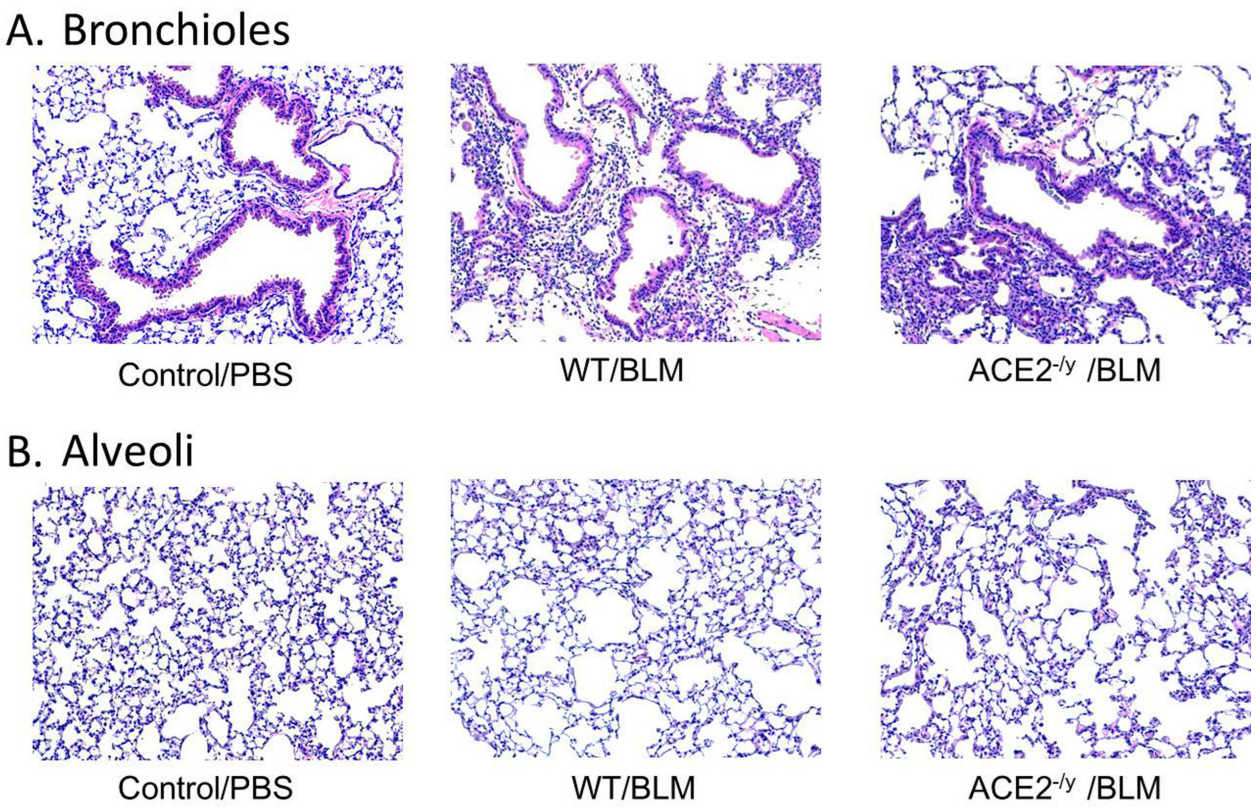

Fig. 2. Pathological Examination Using Hematoxylin and Eosin Stain. The WT and ACE2$^{-/y}$ mice were treated with bleomycin for 3 weeks (WT/BLM and ACE2$^{-/y}$/BLM groups), then were sacrificed and lung tissue was isolated for pathological examination. The hematoxylin and eosin stains of pulmonary bronchiolar (A) and alveoli (B) regions of the mice are shown. Compared to that of the Control/PBS group, infiltration of white blood cells and alveolar damage in the lungs was significantly increased in the mice with bleomycin treatment. Magnification: 10× objective.

(Figure 4A) and IL-6 (Figure 4B) in the WT/BLM mice treated with bleomycin for 3 weeks were approximately 3.5- and 4-fold higher than those in the Control/PBS mice (P<0.01), respectively. In the ACE2$^{-/y}$/BLM mice, the levels of both pulmonary TGF-β1 and IL-6 were significantly higher than those in the WT/BLM mice, by 1.5- and 2.2-fold (P<0.01), respectively (Figure 4).

Pulmonary ACE and ACE2 activities in mice with bleomycin treatment

The activities of pulmonary ACE and ACE2 were investigated to test the hypothesis that RAS mediators could participate in the pathogenic induction of lung injury by bleomycin treatment. The pulmonary ACE activity of the WT/BLM and ACE2$^{-/y}$/BLM mice was significantly increased, by 2- and 5.5-fold, respectively, compared to that in the Control/PBS (P<0.01) mice (Figure 5A). Of note, the ACE activity induced by bleomycin in the lungs of ACE2$^{-/y}$/BLM mice was significantly higher than that in the WT/BLM mice (P<0.01).

Relative ACE2 activity in the lungs of WT/BLM mice was upregulated approximately 1.3-fold after 3 weeks of bleomycin treatment (Figure 5B). However, the pulmonary ACE2 levels

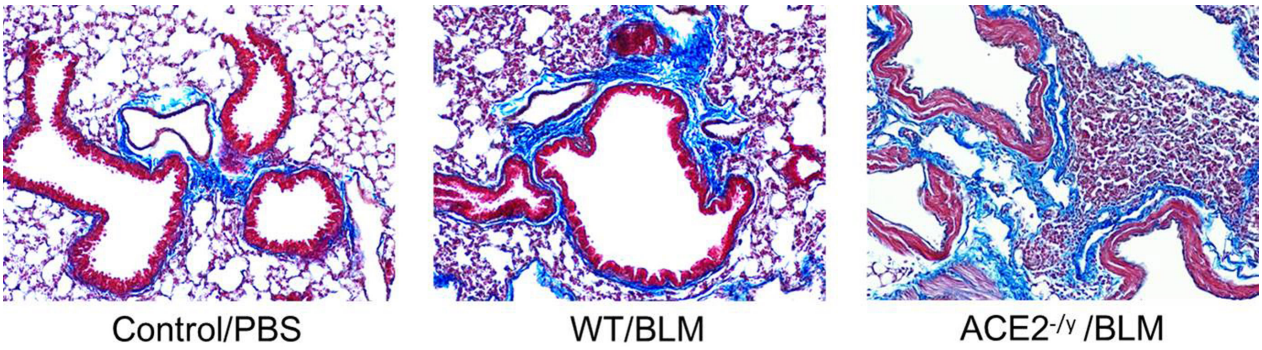

Fig. 3. Pulmonary Pathology Using Masson's Trichrome Stain. The WT and ACE2$^{-/y}$ mice were treated with bleomycin for 3 weeks (WT/BLM and ACE2$^{-/y}$/BLM groups), then were sacrificed and lung tissue was isolated for pathological examination. The Masson's trichrome stains of pulmonary bronchiolar sections of the mice are shown. Compared to that of the Control/PBS group, severe fibrosis (blue-stained) was observed in the lungs of the mice with bleomycin treatment. Magnification: 10× objective.

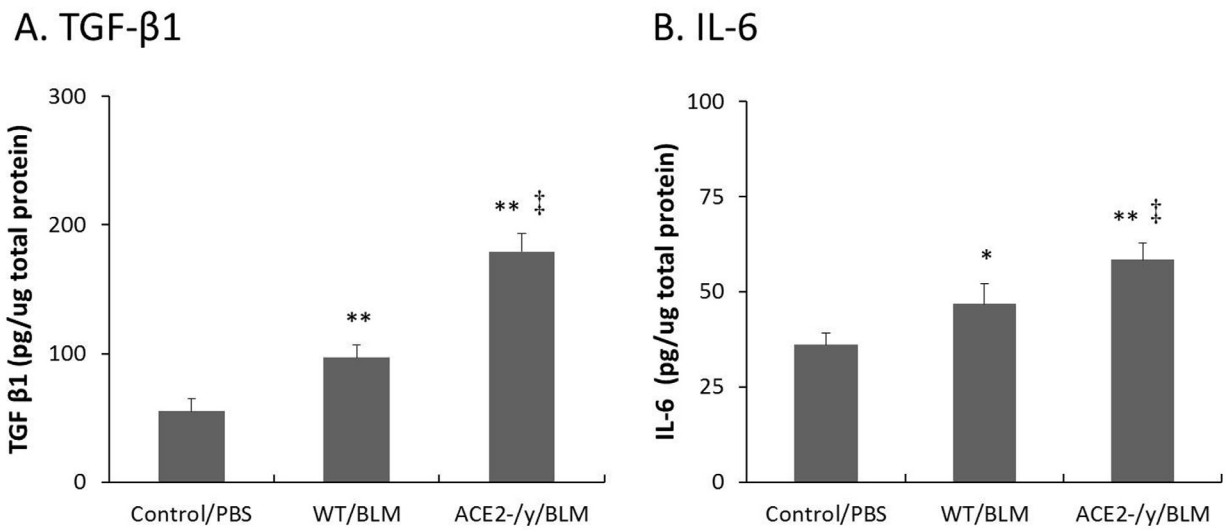

Fig. 4. Pulmonary TGF-β1 and IL-6 Levels in the Mice with Bleomycin Treatment. The WT and ACE2$^{-/y}$ mice were treated with bleomycin for 3 weeks (WT/BLM and ACE2$^{-/y}$/BLM groups), then were sacrificed and lung tissue homogenates were prepared. Transforming growth factor-β1 (TGF-β1, A) and interleukin-6 (IL-6, B) levels in the homogenates were measured using enzyme-linked immunosorbent assay (ELISA) kits. All values are expressed as mean±SD of each group; *P<0.05 and ** P<0.01 compared with the Control/PBS group, $^{‡}P$<0.01 compared with the WT/BLM group.

were not significantly different between the WT/BLM and Control/PBS mice. Any ACE2 activity detected in the ACE2$^{-/y}$/BLM mice was a background value because the ACE2 gene was absent in the knockouts.

Pulmonary fibrosis markers in mice after bleomycin challenge

The lung injury of the mice induced by bleomycin increased the amount of pulmonary cytokines (TGF-β1 and IL-6), which indicates that the bleomycin-induced inflammatory re-

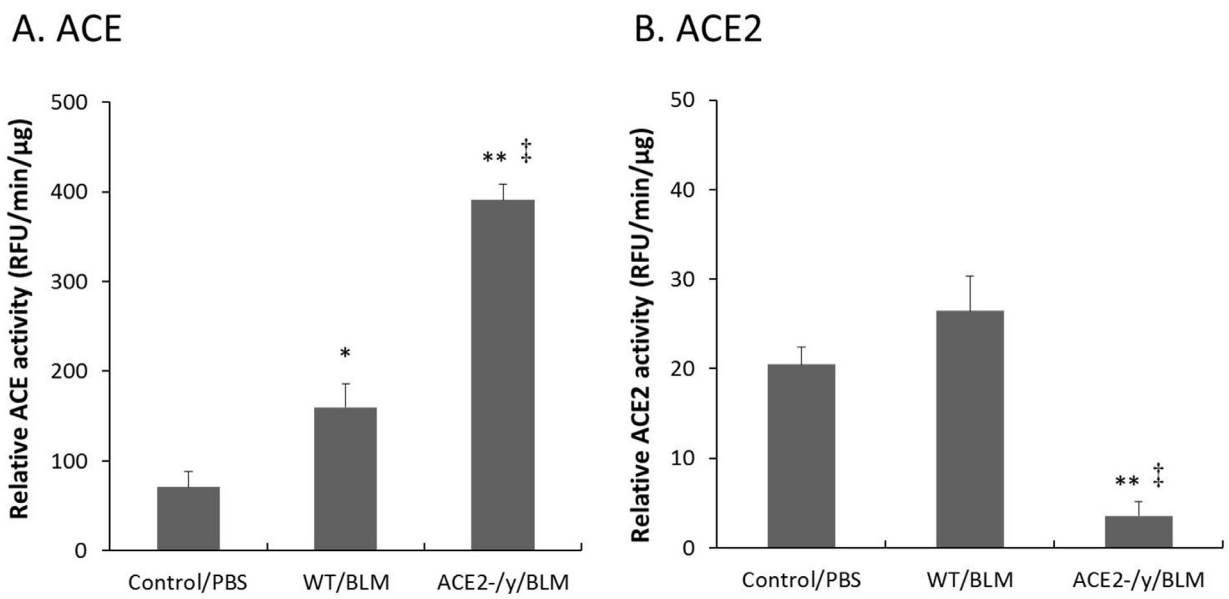

Fig. 5. Pulmonary ACE and ACE2 Activities of the Mice with Bleomycin Treatment. The lung homogenates prepared from the mice were used for the detection of angiotensin-converting enzyme (ACE, A) and ACE 2 (ACE2, B) activity. All values are expressed as mean±SD of each group; **P*<0.05 and ***P*<0.01 compared with the Control/PBS group, ‡*P*<0.01 compared with the WT/BLM group. RFU, relative fluorescence units.

sponse was associated with these cytokines. Western blot assays were performed to further examine whether ACE2 could also affect the pulmonary fibrosis biomarkers, CTGF and elastin, in the injured lungs (Figure 6). The relative pulmonary CTGF expression in the WT/BLM and ACE2$^{-/y}$/BLM mice was upregulated 1.3- and 1.6-fold, respectively, compared with that in the Control/PBS mice (P<0.01) (Figure 6A). In addition, the relative elastin expression in the WT/BLM and ACE2$^{-/y}$/BLM mice was upregulated 1.3- and 1.8-fold, respectively, compared with that in the Control/PBS mice (Figure 6B). The level of CTGF in the ACE2$^{-/y}$/BLM mice was higher than that in the WT/BLM mice (P<0.05). Even though the level of elastin in the ACE2$^{-/y}$/BLM mice was higher than that in the WT/BLM mice, there was no statistically significant difference between them. However, the experimental results show that bleomycin treatment leads to a significant increase in the expression of CTGF and elastin, and that ACE2 deficiency can enhance the expression of both markers.

Discussion

In this study, the major RAS components, ACE and ACE2, pro-inflammatory cytokines, and biomarkers associated with fibrosis in the lung tissue of the bleomycin-treated mice were measured. Our main findings are: (1) increased physiological and pathological changes in the ACE2$^{-/y}$/BLM mice compared with those in the WT/BLM mice, (2) markedly increased pulmonary TGF-β1 and IL-6, which were highest in the ACE2$^{-/y}$/BLM mice, indicating severe inflammation, and (3) that high ACE activity, fibrosis-related CTGF, and elastin expression were associated with bleomycin-induced pul-

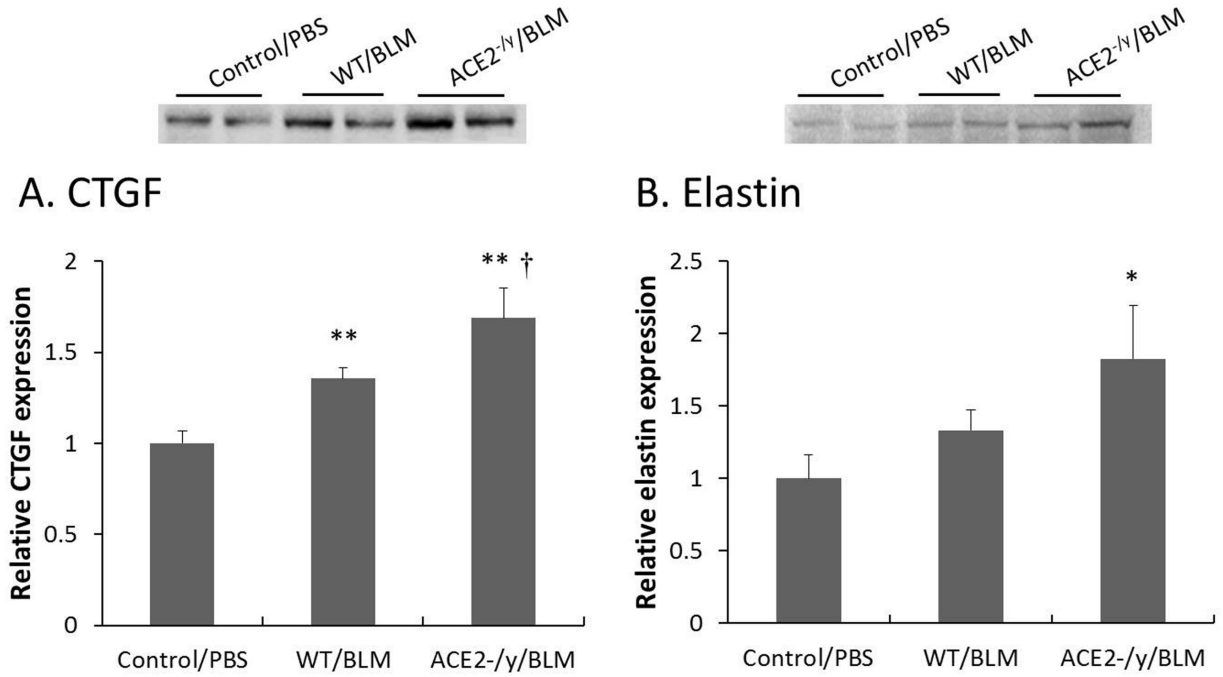

Fig. 6. Pulmonary CTGF and Elastin Levels in the Mice with Bleomycin Treatment. The lung homogenates prepared from the mice were used for the detection of connective tissue growth factor (CTGF A) and elastin (B) levels by western blot. The CTGF and elastin expressions were normalized to their corresponding β-actin levels and were expressed relative to Control/PBS values that were arbitrarily set as 1. Representative western blot images are shown above the corresponding quantification plots. All values are expressed as mean±SD of each group; **P*<0.05 and ***P*<0.01 compared with the Control/PBS group, †*P*<0.05 compared with the WT/BLM group.

monary injury.

TGF-β1 and IL-6 concentrations in the mouse lungs were markedly increased after bleomycin challenge, and their levels in the lungs of ACE2$^{-/y}$/BLM mice were significantly increased compared with those of the WT/BLM group. Previous studies have indicated that TGF-β and IL-6 are associated with various pulmonary diseases, such as asthma, chronic bronchitis, chronic obstructive pulmonary disease (COPD), acute lung injury, and ARDS [17-18]. TGF-β and IL-6 may initially be involved in tissue repair and wound healing, but large amounts of these cytokines may ultimately lead to various inflammatory diseases [19]. It has also been reported that TGF-β plays a central role in the pathogenesis of pulmonary fibrosis. Increased TGF-β and TGF-β receptor expression in the bronchiolar and alveolar epithelium of IPF patients is correlated with lung function decline, histological changes, and collagen-producing fibroblasts in IPF [20]. Our study suggests that TGF-β signaling plays a role in the development and progression of IPF. Studies have shown that IL-6 mediates many inflammatory processes in the lung, and its release has been implicated in the pathogenesis of a variety of respiratory diseases [21-22]. Activated Janus kinases (JAKs) mediate the phosphorylation and activation of the major transcription factor regulated by IL-6. In addition, the IL-6 concentration in bronchoalveolar lavage fluid was found to be 100 times higher than normal in patients with ARDS, when the disease is persis-

tent [21].

Based on our results, we preliminarily conclude that loss of ACE2 induces more severe immune responses. Recent evidence suggests that the RAS has important functions outside of the cardiovascular system. Since ACE2 was identified as a key receptor for the coronavirus infections responsible for SARS [23], major attention has been drawn to the potentially protective role of ACE2 in lung diseases. ACE2 knockout mice exhibited exacerbated lung injury compared with that of WT mice [14]. Loss of ACE2 was shown to cause enhanced vascular permeability, increased lung edema, neutrophil accumulation, and worsened lung function, which shows that the RAS plays an important role in lung injury [24-25]. Of importance, the experiments also revealed that ACE2 is an essential receptor for SARS infections *in vitro* and *in vivo* [23]. Additional evidence confirming that ACE2 is central to pulmonary endothelial and epithelial functions includes: (1) ACE2 is abundantly expressed in the pulmonary endothelium [26-27], (2) ACE2 is significantly decreased in lung biopsies of patients with IPF [27], and (3) bleomycin-induced pulmonary fibrosis is associated with a decrease in ACE2 activity [27].

The findings in our study are similar to those of previous studies. In our study, the relative ACE activity of the lungs in WT and ACE2$^{-/y}$ mice was significantly upregulated by bleomycin challenge. ACE activity in the ACE2$^{-/y}$ mice was significantly higher than that in the WT mice. The increase in ACE activity might lead to increased Ang II levels, which would affect the blood vessels and cause inflammation. From the above results, we conclude that ACE2 could degrade Ang II, to form Ang-(1-7) and, combined with activation of the Mas receptor, reduce inflammatory responses. Therefore, in ACE2-deficient mice, excessive Ang II would combine with Ang II type 1 receptor (AT1R) to induce more inflammatory responses, abnormal pulmonary vasoconstriction and vascular remodeling. Of importance, treatment with catalytically active recombinant ACE2 protein improved the symptoms of acute lung injury in both WT and ACE2 KO mice [14]. It is noteworthy that lung injury in experimental ARDS in mice can be attenuated by blocking the RAS [14]. One complication of ARDS is lung fibrosis. Li *et al*. [27] have demonstrated that ACE2 mRNA and activity are downregulated in human and experimental lung fibrosis, which suggests that ACE2 limits the local accumulation of Ang II.

In the fibrotic process, CTGF is also an important mediator of tissue remodeling and fibrosis. CTGF is a secreted, matricellular protein with very complex biological activity. It has been proven to regulate many signaling pathways, leading to cell adhesion and migration, angiogenesis, myofibroblast activation, and extracellular matrix deposition and remodeling, which cumulatively cause tissue remodeling and fibrosis [28]. CTGF can upregulate a variety of cytokines, such as TGF-β [29] and vascular endothelial growth factor [30], both of which can induce expression of CTGF. Therefore, CTGF can promote fibrosis in a positive feedback loop. Pulmonary fibrosis is a progressive pathological process, characterized by fibroblast differentiation, excessive extracellular matrix deposition, and gradual loss of lung function. The deposited extracellular matrix is composed of both collagen and elastin. Therefore, we examined the expression of elastin in the lungs after bleomycin challenge.

Conclusion

Our results showed the hallmark features of bleomycin-induced lung disease. Weight loss, increased RRR, and pulmonary inflammation were induced within 1 week in the WT and ACE2$^{-/y}$ mice after bleomycin treatment, providing opportunities to test therapeutic targets for disease induction and progression. In histological sections, we also observed that the bleomycin-induced pulmonary injury in the ACE2$^{-/y}$ mice was faster and more severe than that in the WT mice. Therefore, we conclude that ACE2 plays an important role in influencing the pathological changes induced by bleomycin. However, the molecular mechanisms of the RAS-dependent pathway that are responsible for the disease pathology have yet to be explored.

Acknowledgements

This work was supported by a grant (MOST 104-2313-B-009-001-MY3) from the Ministry of Science and Technology (MOST), Taiwan. This work was also supported by grants from Hsinchu Mackay Memorial Hospital, Taiwan (MMH-CT-10503 and MMH-HB-10507).

References

1. Moeller A, Ask K, Warburton D, *et al*. The bleomycin animal model: a useful tool to investigate treatment options for idiopathic pulmonary fibrosis? Int J Biochem Cell Biol 2008; 40: 362-82.
2. Thannickal VJ, Toews GB, White ES, *et al*. Mechanisms of pulmonary fibrosis. Annu Rev Med 2004; 55: 395-417.
3. Hao Y, Liu Y. Osthole alleviates bleomycin-induced pulmonary fibrosis via modulating angiotensin-converting enzyme 2/angiotensin-(1-7) axis and decreasing inflammation responses in rats. Biol Pharm Bull 2016; 39: 457-65.
4. Okamoto A, Nojiri T, Konishi K, *et al*. Atrial natriuretic peptide protects against bleomycin-induced pulmonary fibrosis via vascular endothelial cells in mice: ANP for pulmonary fibrosis. Respir Res 2017; 18: 1.
5. Kuwano K, Hagimoto N, Hara N. Molecular mechanisms of pulmonary fibrosis and current treatment. Curr Mol Med 2001; 1: 551-73.
6. King TE Jr., Pardo A, Selman M. Idiopathic pulmonary fibrosis. Lancet 2011; 378: 1949-61.
7. Yao HW, Zhu JP, Zhao MH, *et al*. Losartan attenuates bleomycin-induced pulmonary fibrosis in rats. Respiration 2006; 73: 236-42.
8. Waseda Y, Yasui M, Nishizawa Y, *et al*. Angiotensin II type 2 receptor antagonist reduces bleomycin-induced pulmonary fibrosis in mice. Respir Res 2008; 9: 43.
9. Pan CH, Wen CH, Lin CS. Interplay of angiotensin II and angiotensin (1-7) in the regulation of matrix metalloproteinases of human cardiocytes. Exp Physiol 2008; 93: 599-612.
10. Hsieh WY, Kuan TC, Cheng KS, *et al*. ACE/ACE2 ratio and MMP-9 activity as potential biomarkers in tuberculous pleural effusions. Int J Biol Sci 2012; 8: 1197-205.
11. Hung YH, Hsieh WY, Hsieh JS, *et al*. Alternative roles of STAT3 and MAPK signaling pathways in the MMPs activation and progression of lung injury induced by cigarette smoke exposure in ACE2 knockout mice. Int J Biol Sci 2016; 12: 454-65.
12. Kuba K, Imai Y, Penninger JM. Angiotensin-converting enzyme 2 in lung diseases. Curr Opin Pharmacol 2006; 6: 271-6.
13. Montes E, Ruiz V, Checa M, *et al*. Renin is an angiotensin-independent profibrotic mediator: role in pulmonary fibrosis. Eur Respir J 2012; 39: 141-8.
14. Imai Y, Kuba K, Penninger JM. The discovery of angiotensin-converting enzyme 2 and its role in acute lung injury in mice. Exp Physiol 2008; 93: 543-8.
15. Kuan TC, Yang TH, Wen CH, *et al*. Identifying the regulatory element for human angiotensin-converting enzyme 2 (ACE2) expression in human cardiofibroblasts. Peptides 2011; 32: 1832-9.
16. Vickers C, Hales P, Kaushik V, *et al*. Hydrolysis of biological peptides by human angiotensin-converting enzyme-related carboxypeptidase. J Biol Chem 2002; 277: 14838-43.
17. Barnes PJ. The cytokine network in asthma and chronic

obstructive pulmonary disease. J Clin Invest 2008; 118: 3546-56.
18. Rincon M, Irvin CG. Role of IL-6 in asthma and other inflammatory pulmonary diseases. Int J Biol Sci 2012; 8: 1281-90.
19. Ganeshan K, Johnston LK, Bryce PJ. TGF-β1 limits the onset of innate lung inflammation by promoting mast cell-derived IL-6. J Immunol 2013; 190: 5731-8.
20. Kisseleva T, Brenner DA. Hepatic stellate cells and the reversal of fibrosis. J Gastroenterol Hepatol 2006; 21: S84-7.
21. Park CS, Chung SW, Ki SY, *et al*. Increased levels of interleukin-6 are associated with lymphocytosis in bronchoalveolar lavage fluids of idiopathic nonspecific interstitial pneumonia. Am J Respir Crit Care Med 2000; 162: 1162-8.
22. Park WY, Goodman RB, Steinberg KP, *et al*. Cytokine balance in the lungs of patients with acute respiratory distress syndrome. Am J Respir Crit Care Med 2001; 164: 1896-903.
23. Li W, Moore MJ, Vasilieva N, *et al*. Angiotensin-converting enzyme 2 is a functional receptor for the SARS coronavirus. Nature 2003; 426: 450-4.
24. Jeffery TK, Wanstall JC. Comparison of pulmonary vascular function and structure in early and established hypoxic pulmonary hypertension in rats. Can J Physiol Pharmacol 2001; 79: 227-37.
25. Mandegar M, Fung YC, Huang W, *et al*. Cellular and molecular mechanisms of pulmonary vascular remodeling: role in the development of pulmonary hypertension. Microvasc Res 2004; 68: 75-103.
26. Wiener RS, Cao YX, Hinds A, *et al*. Angiotensin converting enzyme 2 is primarily epithelial and is developmentally regulated in the mouse lung. J Cell Biochem 2007; 101: 1278-91.
27. Li X, Molina-Molina M, Abdul-Hafez A, *et al*. Angiotensin converting enzyme-2 is protective but downregulated in human and experimental lung fibrosis. Am J Physiol Lung Cell Mol Physiol 2008; 295: L178-85.
28. Lipson KE, Wong C, Teng YC, *et al*. CTGF is a central mediator of tissue remodeling and fibrosis and its inhibition can reverse the process of fibrosis. Fibrogenesis Tissue Repair 2012; 5(Suppl 1): S24.
29. Yang H, Huang Y, Chen X, *et al*. The role of CTGF in the diabetic rat retina and its relationship with VEGF and TGF-beta, elucidated by treatment with CTGFsiRNA. Acta Ophthalmol 2010; 88: 652-9.
30. Liu Y, Xiao L, Peng YM, *et al*. Inhibition effect of small interfering RNA of connective tissue growth factor on the expression of vascular endothelial growth factor and connective tissue growth factor in cultured human peritoneal mesothelial cells. Chin Med J. (Engl) 2007; 120: 231-6.

第二型血管收縮素轉換酶於 bleomycin 誘發肺部纖維化病變機轉中之角色探討

謝文郁 *,**** 謝日升 ** 莊婉暄 *** 林志生 ** 黃呈誼 *

背景：博萊黴素 (bleomycin) 治療癌症造成間質性肺炎或肺纖維化，與腎素－血管收縮素系統 (Renin-angiotensin system; RAS) 調節密切相關。第二型血管收縮素轉換酶 (Angiotensin-converting enzyme 2; ACE2) 可水解血管收縮素 II (Angiotensin II; Ang II)，本研究為探討 bleomycin 誘發肺損傷與 ACE2 的關聯。

方法：雄性野生型 (WT; C57BL/6)、ACE2 基因剔除 (ACE2 KO；$ACE2^{-/y}$) 小鼠由氣管給予 bleomycin，每週量測體重和呼吸次數 (resting respiratory rate; RRR) 後犧牲並採集肺臟進行生化與病理分析。

結果：比較 bleomycin 處理後 WT 與 $ACE2^{-/y}$ 小鼠。RRR 上升、肺臟中白血球浸潤、纖維化病變、tumor growth factor beta 1 (TGF-β1)、interleukin-6 (IL-6)、ACE 活性及結締組織生長因子 (CTGF) 和彈性蛋白 (elastin) 在 $ACE2^{-/y}$ 小鼠均有顯著高表現。

結論：Bleomycin 可誘發肺部發炎反應、纖維化及 ACE 活性上升，與 ACE2 缺失的 RAS 有關，導致 Ang II 濃度提升加劇損傷。推測 RAS 的調節可減緩 bleomycin 誘發肺部炎症反應的損傷。*(胸腔醫學* ***2018; 33: 50-62)***

關鍵詞：博萊黴素，肺纖維化，腎素－血管收縮素系統，第二型血管收縮素，炎症反應

* 新竹馬偕紀念醫院　內科部　胸腔內科，** 國立交通大學　生物科技學系
*** 新竹馬偕紀念醫院　內科部　呼吸治療科，**** 明新科技大學　老人服務事業管理系
索取抽印本請聯絡：黃呈誼醫師，新竹馬偕紀念醫院　內科部　胸腔內科，300 新竹市東區光復路二段 690 號

Clinical Experiences in the Management of Upper Airway Injury

Che-Chih Cheng, Chin-Chieh Hsu, Jen-Chih Chen

Airway trauma, also known as tracheobronchial injury, is a cause of immediate death after an accident. For this report, we collected the medical records of 4 patients with upper airway injuries: 1. a patient with blunt chest trauma with tracheal laceration due to a traffic accident; 2. a patient with severance of the larynx by due to a knife wound; 3. a patient with a penetrating injury to the neck with partial transection of the trachea by a knife; and 4. a patient with a penetrating injury to the right upper neck by the metal lock of his helmet in a traffic accident. Our management of these patients involved, conservative treatment with a hand-made tracheostomy tube (a modified endotracheal tube) in patient 1 and surgical repair with absorbable sutures interruptedly in the others. Patient 1 was weaned from the ventilator after 34 days, patient 2 after 8 days, patient 3 after 2 days, and patient 4 after 1 day. All the patients with upper airway injuries survived after our treatment and there was no further complication. ***(Thorac Med 2018; 33: 63-69)***

Key words: upper airway injury, tracheobronchial injury

Introduction

Airway trauma, also known as tracheobronchial injury (TBI), is a cause of immediate death after an accident. The incidence of TBI among the victims with chest and neck injuries is about 0.5-2% [1], and the incidence of tracheal rupture after endotracheal intubation ranges from 0.05% to 0.37% [2]. The mortality rate due to traumatic TBI has gradually decreased, from 36% in 1950, to 30% in 1966, and 9% in 2001 [2]. Generally speaking, the mechanisms of TBI are penetrating trauma, the most common, and blunt trauma which includes neck hyperextension and direct blows. Depending on the site and severity of injury, we may observe compatible or possible symptoms and signs of TBI, but most of them are not specific [2]. Early diagnosis and prompt treatment can increase the survival rate and reduce mortality and the complication rate [3]. Here, we report our clinical practice experiences in the management of upper airway injury in recent years.

Case Presentation

Patient 1, a 67-year-old man, suffered from blunt chest trauma with multiple fractures of bi-

Division of Thoracic Surgery, Department of General Surgery, Kaohsiung Armed Forces General Hospital
Address reprint requests to: Dr. Jen-Chih Chen, Division of Thoracic Surgery, Department of General Surgery, Kaohsiung Armed Forces General Hospital, No. 2, Zhongzheng 1st Rd., Lingya Dist., Kaohsiung City 802, Taiwan (R.O.C.)

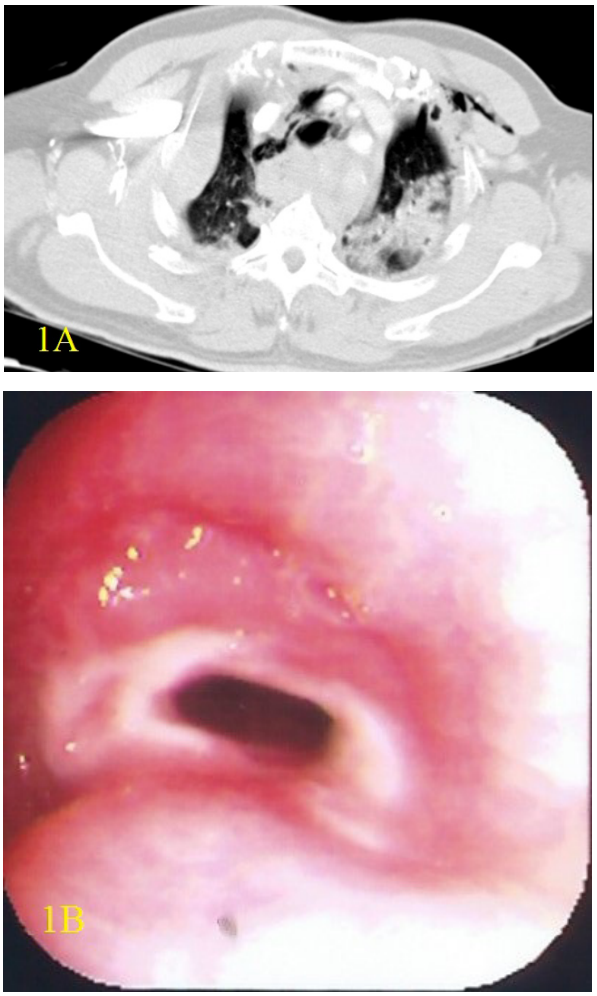

Fig. 1. Images of patient 1. A: Computed tomography of the chest showed pneumomediastinum; B: Perioperative bronchoscopy showed granulation formation in the laceration wound

lateral ribs, pneumomediastinum, and bilateral hemopneumothorax after a traffic accident (Figure 1A). He underwent emergency intubation of an endotracheal tube (ETT) and chest tubes for resuscitation because of shock status and acute respiratory failure. Progressive hypoxia was noted 2 days later, and a tracheal laceration, about 1 cm in length between the 3rd and 4th ring, was diagnosed by bronchoscopy. He was given conservative treatment with an ETT cuff bypassing the laceration wound. Due to respiratory failure with mechanical ventilator (MV) dependence, a tracheostomy was performed above the laceration wound 2 weeks later, and a hand-made long tracheostomy tube, a modified ETT, was inserted to bypass the laceration wound (proximal cuff edge was about 1 cm below the tracheostomy wound). Mild granulation tissue formation in the laceration wound was found by perioperative bronchoscopy (Figure 1B). The patient was successfully weaned from MV 34 days later, and the tracheostomy tube was removed 181 days later.

Patient 2, a 61-year-old woman, suffered from a cutting injury to the left neck with leakage of air and critical hemorrhage. She received emergency ETT intubation straight through the larynx laceration to maintain her airway. The operative findings were: 1. severance of the larynx, lower portion, with respiratory failure, and 2. severance of the external jugular vein (EJV) and rupture of the internal jugular vein (IJV), left, with hemorrhagic shock. She underwent emergency surgery with tracheostomy, interrupted repair of the larynx with 4-0 absorbable sutures, repair of the IJV, and reconstruction of the EJV, left. She was successfully weaned from MV 8 days later, and the tracheostomy tube was removed 37 days later. Although limited movement of the right vocal cord and a fixed position (medial) of the left vocal cord were noted by laryngoscopy in the outpatient department (OPD) 24 days later (Figure 2A), functioning of the patient's bilateral vocal cords totally recovered about 6 months later with conservative treatment (Figure 2B).

Patient 3, a 20-year-old man, suffered a deep penetrating injury to the left lower neck (near the sternoclavicular joint) by a knife. The operative findings were: 1. a penetrating injury to the left neck with partial disruption of the trachea (more than 180° circumferential lac-

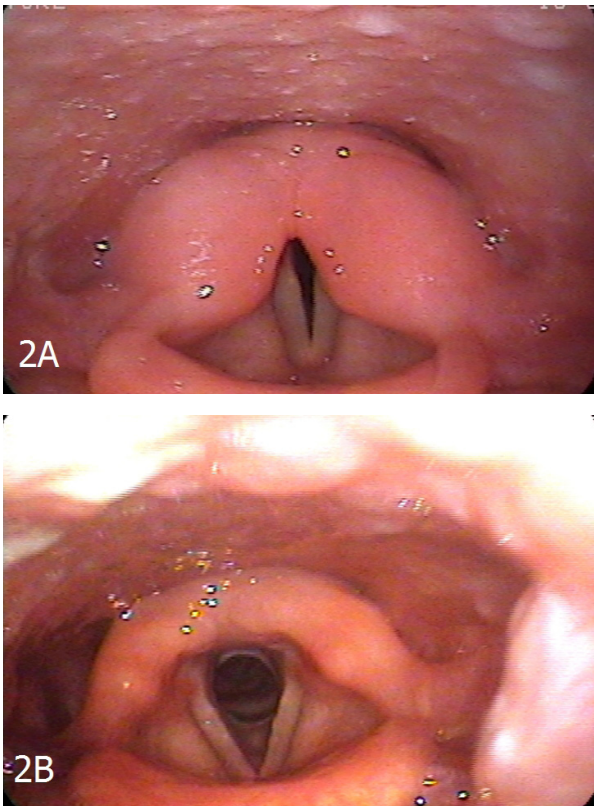

Fig. 2. Laryngoscopy images of patient 2. A: 24 days after trauma (limited movement); B: 6 months after trauma (normal activity)

eration at the thyroid level) (Figure 3) and 2. right pneumothorax and pneumomediastinum. The patient's trachea was repaired with a 3-0 absorbable suture interruptedly and he was successfully weaned from the ETT 2 days later.

Patient 4, a 20-year-old man, suffered a penetrating injury to the right upper neck by the metal lock of his helmet in a traffic accident. Pneumomediastinum was noted in a computed tomography (CT) scan of his chest (Figure 4). During operation, laryngeal laceration with airway compromise was suspected, and the patient received emergency temporary tracheostomy and complicated laryngoplasty with a 3-0 absorbable suture interruptedly. He was successfully weaned from MV 1 day later, and the tracheostomy tube was removed 20 days later.

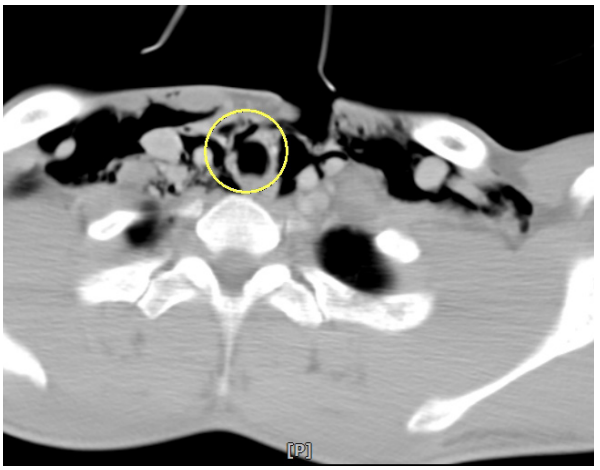

Fig. 3. Computed tomography of the neck of patient 3 showed deep penetrating injury with tracheal laceration

Fig. 4. Computed tomography of the chest of patient 4 showed pneumomediastinum

All of the patients with upper airway injuries survived after treatment, and there were no further complications authenticated by laryngoscopy, bronchoscopy, CT scan, and pulmonary function test during follow-up at the OPD. Clinical data from medical records were reviewed retrospectively (Table 1).

Table 1. Patients' Characteristics

Patient	Gender	Age	Mechanism	Procedure	Operative findings	Complications
1	Male	67	BCT	ETT bypass	Laceration of anterior wall of trachea, about 1 cm between the 3rd and 4th ring	Nil
2	Female	61	Cutting injury	Primary repair	Severance of larynx, lower portion, about 5 cm	Limited movement of bilateral vocal cords, but recovery 6 months later
3	Male	20	Penetrating injury	Primary repair	Partial disruption of trachea (more than 180° circumferential laceration at thyroid level)	Nil
4	Male	20	Penetrating injury	Primary repair	Larynx laceration, about 2 cm	Nil

BCT: blunt chest trauma; ETT: endotracheal tube

Discussion

TBI can occur due to penetrating injury, neck hyperextension, or direct blows [2]. The severity of penetrating injury is related to its depth and involved organs. Neck hyperextension can cause tracheal tears, paramedian vertical fractures of the larynx and trachea, and/or even complete laryngotracheal separation. Direct blows may cause thyroid and cricoid cartilage injury [2].

We can observe compatible or possible symptoms and signs in victims of TBI based on the site and severity of injury, but most of the symptoms and signs are not specific. Common symptoms and signs include subcutaneous emphysema (~87%) [4], dyspnea/tachypnea/respiratory distress (59~100%), hemoptysis (~74%), subcutaneous emphysema (~87%), pneumothorax (17~70%), voice change, and vessel injuries [5-7]. Bronchoscopy and CT scans are used to reach a definitive diagnosis [8].

The first and most important step in the management of TBI is establishing airway patency, and endotracheal intubation is usually performed. ETT intubation with a bronchoscope under spontaneous breathing is recommended [1,9]. The tube's cuff needs to bypass the lesion because positive pressure ventilation may increase the air leak and lead to severe respiratory insufficiency [10]. Insertion of a tracheostomy tube through the wound would be the best way to manage patients with cervical penetration, and tracheostomy should be performed in every patient with TBI after failed ETT intubation [11].

The principles of surgical management are as follows [2]:

- Close the airway defect of airway to improve ventilation.
- Prevent from mediastinal spillage and infection.
- Avoid spontaneous healing complications that can lead to stenosis of the air-

way and recurrent pulmonary infection.

Surgical intervention techniques include direct sutures for small tears/lacerations, debridement of the infected/devitalized tissues, trimming the edges of the injured airway, and end-to-end anastomosis for complete/partial disruption. Advanced debridement or mobilization around the injured airway should be avoided as it may increase the possibility of neurovascular injury [12]. It is rarely necessary to explore and assess the recurrent laryngeal nerves because the involved vocal cords, or at least 1 vocal cord, would recover partial or intact function within several months [2].

However, we would choose conservative treatment if the patients' characters met the criteria as below [13]:

- Small laceration (<2 cm)
- The ETT cuff or tracheostomy tube distally bypassed the lesion
- Adequate ventilation with PEEP and low tidal volumes
- No increasing subcutaneous emphysema after chest tube intubation with suction
- No signs of ongoing infection.

We chose conservative or surgical treatment for our patients based on their respective wound status, and there were no further complications during follow-up exams at the OPD.

Conclusion

Based on our clinical experience in the management of upper airway injury, maintenance of airway patency is the first and most important step. Then, we would choose to implement a prompt therapeutic plan, conservative treatment or surgical procedures, according to the above-stated criteria, to increase the recovery rate and reduce the incidence of complications. The aims of surgical intervention are: 1. restore the integrity of the airway, 2. minimize the loss of pulmonary parenchyma, 3. maintain vocal function, and 4. avoid permanent tracheostomy [2]. We would choose conservative methods, usually an ETT/tracheostomy tube cuff distally bypassing the lesion, to manage TBI patients if the above criteria are met.

References

1. Riley RD, Miller PR, Meredith JW, *et al*. Injury to the esophagus, trachea and bronchus. In: Moore EE, Feliciano DV, Mattox KL, ed. Trauma. 5th ed. New York: McGraw-Hill, 2004; 539-52.
2. Prokakis C, Efstratios NK, Panagiotis D, *et al*. Airway trauma: a review on epidemiology, mechanisms of injury, diagnosis and treatment. Journal of Cardiothoracic Surgery 2014; 9: 117.
3. Chagnon FP, Mulder DS. Laryngotracheal trauma. Chest Surg Clin N Am 1996; 6: 733-48.
4. Koletsis E, Prokakis C, Baltayiannis N, *et al*. Surgical decision making on the basis of clinical evidences and the injury's anatomical setting. Injury 2012; 43: 1437-41.
5. Kelly JP, Webb WR, Moulder PV, *et al*. Management of airway trauma I: tracheobronchial injuries. Ann Thorac Surg 1985; 40: 551-5.
6. Baumgartner F, Sheppard B, De Virgilio C, *et al*. Tracheal and main bronchial disruptions after blunt chest trauma: presentation and management. Ann Thorac Surg 1990; 50: 569-74.
7. Barmada H, Gibbons JR. Tracheobronchial injury in blunt and penetrating chest trauma. Chest 1994; 106: 74-8.
8. Scaglione M, Romano S, Pinto A, *et al*. Acute tracheobronchial injuries: Impact of imaging on diagnosis and management implications. Eur J Radiol 2006; 59: 336-43.
9. Cassada DC, Munyikwa MP, Moniz MP, *et al*. Acute injuries of the trachea and main bronchi: importance of early diagnosis. Ann Thorac Surg 2000; 69: 1563-7.
10. Corneille MG, Stewart RM, Cohn SM, *et al*. Upper air-

way injury and its management. Semin Thorac Cardiovasc Surg 2008; 20: 8-12.
11. Wu MH, Tsai YF, Lin MY, *et al*. Complete laryngotracheal disruption caused by blunt injury. Ann Thorac Surg 2004; 77: 1211-5.
12. Dougenis D. Trauma of the tracheobronchial tree. Arch Hellen Med 2002; 19: 258-69.
13. Kiser AC, O'Brien SM, Detterbeck FC, *et al*. Blunt tracheobronchial injuries: treatment and outcomes. Ann Thorac Surg 2001; 71: 2059-65.

上呼吸道損傷之臨床處理經驗

鄭哲智　許晉杰　陳仁智

上呼吸道損傷係創傷後立即死亡的原因之一，且其發生率約佔胸頸創傷患者的 0.5-2%。而呼吸道的保護是處理氣道損傷患者的首要步驟，通常是採用氣管內管插管的方式，也建議利用支氣管鏡導引，以越過病灶處來進行插管。我們收集了四位氣道損傷的患者：1. 車禍導致胸部挫傷併氣管撕裂傷；2. 水果刀造成的喉部切割傷；3. 美工刀造成的頸部穿刺傷及部分氣管截斷；4. 車禍中遭安全帽扣環拉扯造成的上頸部穿刺傷。

我們的臨床處理方式如下：個案 1 採保守治療合併使用自製的加長型氣切管 (改造之氣管內管)；其餘三個個案皆採用可吸收線來進行氣道損傷的修補。四個個案脫離呼吸機的時間依序分別為 34 天、8 天、2 天及 1 天。

在我們的治療後，全部患者皆順利存活，並且在門診追蹤安排的支氣管鏡、電腦斷層或是肺功能中，皆無發現後續的併發症。*(胸腔醫學* ***2018; 33: 63-69)***

關鍵詞：氣道損傷，上呼吸道損傷

國軍高雄總醫院　外科部　胸腔外科
索取抽印本請聯絡：陳仁智醫師，國軍高雄總醫院　外科部　胸腔外科，高雄市苓雅區中正一路 2 號

IgG4-Related Lung Disease in a Patient with Systemic Lupus Erythematosus: A Case Report

Lih-Chyun Chang, Cheng-Han Wu*, Chia-Lin Hsu, Jin-Yuan Shih, Chong-Jen Yu

IgG4-related lung disease (IgG4-RLD) is an uncommon clinicopathological entity. It is a pulmonary manifestation of IgG4-related disease. Lymphadenopathy of IgG4-RLD makes it difficult to distinguish from lung cancer. We report a 67-year-old male patient with IgG4-RLD and systemic lupus erythematosus. His initial presentations in the health examination were an elevated serum creatinine level, anemia, leukopenia and lung tumor. Abdominal magnetic resonance imaging showed marked swelling at the pancreatic head and multiple wedge-shaped lesions in both kidneys. The video-assisted thoracic surgery wedge resection lung specimen had features that met all histologic diagnostic criteria for IgG4-RLD. Under corticosteroid and azathioprine treatment, the serum IgG4 level, renal function and pancreatic lesion improved gradually. When IgG4-RLD is suspected clinically, the serum IgG4 level measurement and surgical lung biopsy are important diagnostic tools. ***(Thorac Med 2018; 33: 70-75)***

Key words: IgG4-related lung disease, systemic lupus erythematosus

Introduction

Attention has been focused on immunoglobulin G4-related diseases (IgG4-RD) recently, but only sporadically. IgG4-RD can affect multiple organs, and they share similar pathologic, serologic, and clinical features. IgG4-related lung disease (IgG4-RLD) can be considered an IgG4-related sclerosing inflammation that shows various types of pulmonary manifestations. Most patients would be recognized as having lung cancer initially. The small size of the specimens from computed tomography (CT)-guided biopsy, bronchoscopic biopsy or lymph node biopsy would not be able to provide adequate evidence of all of these histologic features. We report a 67-year-old man with IgG4-RLD and systemic lupus erythematosus (SLE). Using video-assisted thoracic surgery (VATS) wedge resection, the lung specimen was large enough to meet all histologic diagnostic criteria. With corticosteroid and azathioprine treatment, the serum IgG4 level, renal function and pancreatic lesion improved gradually.

Division of Pulmonary Medicine, *Division of Immunology, Rheumatology and Allergy, Department of Internal Medicine, National Taiwan University Hospital and National Taiwan University College of Medicine, Taipei, Taiwan
Address reprint requests to: Dr. Chia-Lin Hsu, Division of Pulmonary Medicine, Department of Internal Medicine, National Taiwan University Hospital, Taipei, Taiwan, No. 7, Chung-Shan South Road, Taipei, Taiwan

Case Report

This 67-year-old man was a never-smoker. He had a history of hypertension without medical control. His father had died from lung cancer. Because of anemia, leukopenia and an elevated serum creatinine level in a health examination, he was hospitalized at a regional hospital for suspected multiple myeloma. Serum protein electrophoresis showed elevated beta-2 globulin and polyclonal gammopathy (serum IgG: 5,994.0 mg/dL). Bone marrow biopsy showed no evidence of multiple myeloma. However, chest CT revealed a 3.9-cm spiculated mass at the right lower lobe that spread along the major fissure with perifocal interlobular thickening (Figure 1). Aortopulmonary and left paratracheal lymphadenopathies were also noted. He then visited our hospital for further evaluation.

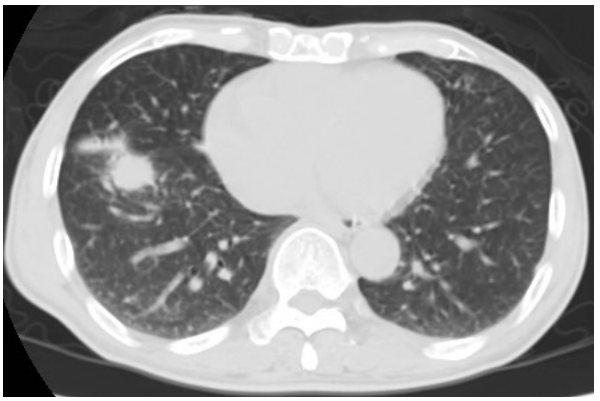

Fig. 1. Chest computed tomography revealed a spiculated ovoid solitary mass in the right lower lobe adhesive to the interlobar fissure.

After admission, he received CT-guided biopsy; pneumothorax occurred during the first sampling. The pathology showed small pieces of soft tissue with lymphocytes and anthracosis in the microscopic exam. No evidence of malignancy was found. Due to suboptimal sampling and that pulmonary malignancy could not be excluded, he underwent VATS wedge resection at the junction between the right upper lobe and the right lower lobe 11 days later. Pathology revealed chronic sclerosing inflammation with abundant plasma cells and small lymphocytes infiltration into the fibrotic lung parenchyma. Storiform fibrosis (Figure 2A) and obliterative phlebitis (Figure 2B) were evident. The pleura was thickened. The immunohistochemical exam revealed that IgG4-positive plasma cells were up to 226/high power fields (HPF), and that IgG4/IgG was more than 95% (Figure 2C). This was compatible with an IgG4-RLD. Laboratory data revealed high serum IgG (3,810 mg/dL) and IgG4 (2,390 mg/dL) levels. Elevated amylase (300 U/L) and lipase (381 U/L) were also found. Besides leukopenia (white blood cells (WBC) 1,600/μL), anemia (9.8 g/dL) and renal insufficiency (blood urea nitrogen (BUN) 21.4 mg/dL, creatinine (Cr) 1.7 mg/dL) were also noted. Abdominal magnetic resonance imaging (MRI) showed marked swelling at the pancreatic head with a decrease in enhancement, and multiple wedge-shaped hypo-enhanced regions in both kidneys (Figure 3A, B), which were compatible with IgG4-RD with pancreatic and renal involvement. After discussion with the rheumatologist, we started steroid and azathioprine treatment (prednisolone 15 mg BID, azathioprine 25 mg QD). SLE was later diagnosed based on clinical and immunologic criteria (leukopenia, anti-nuclear antibody (ANA) 1:80, low complement levels, positive direct Coombs' test and positive antiphospholipid antibody) at the outpatient department. After 6 months' treatment, the serum IgG and IgG4 levels had decreased to 830 mg/dL and 240 mg/dL, respectively. The WBC count, and BUN and Cr levels had also returned to normal. The follow-

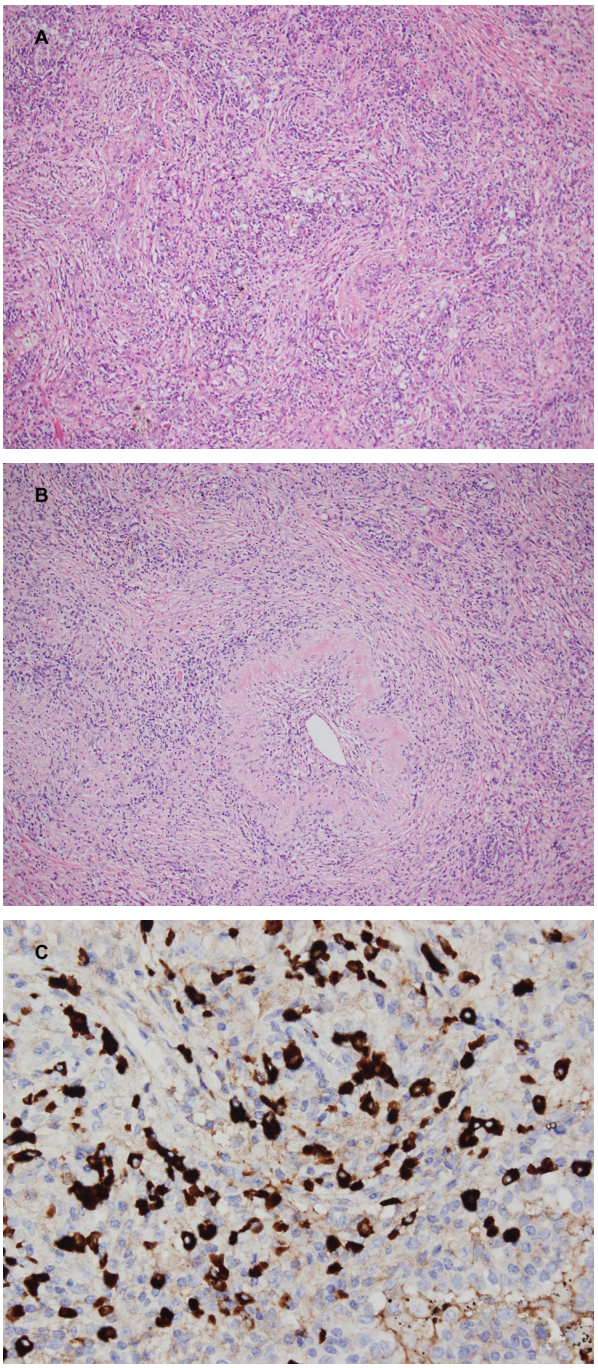

Fig. 2. Histologic finding showed storiform fibrosis (A), and obliterative phlebitis (B). Immunostaining of IgG4 revealed IgG4-positive plasma cells (C).

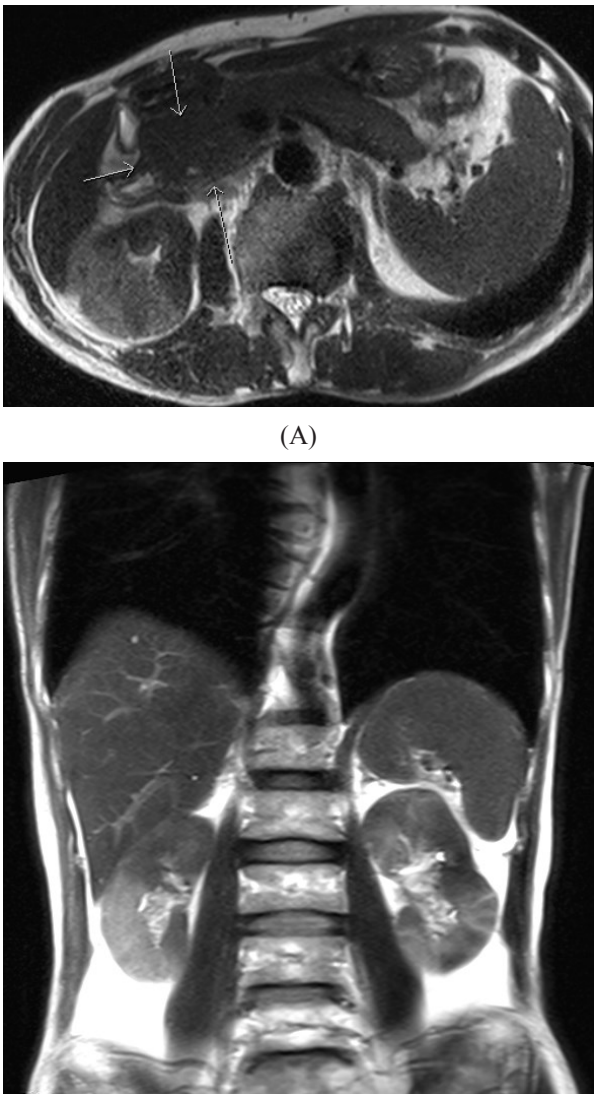

(A)

(B)

Fig. 3. Abdominal magnetic resonance imaging showed swelling at the pancreatic head (A, white arrow) and multiple wedge-shaped hypo-enhanced regions in both kidneys (B).

up abdominal MRI revealed the pancreatic swelling had resolved, and the bilateral kidney lesions were stable. The patient has been kept under treatment with prednisolone, azathioprine and rituximab maintenance therapy for disease control.

Discussion

The first case of IgG4-RD, presenting as

sclerosing pancreatitis with high serum IgG4 concentrations, was reported in 2001 [1]; thereafter, IgG4-related lesions involving other organs were identified. In 2004, 2 patients with autoimmune pancreatitis and lung lesions manifesting as organizing and interstitial pneumonia, respectively, were reported [2-3]. Pulmonary involvement occurs in 12-15% of patients with IgG4-RD [4]. The average age of an IgG4-RLD patient is 69 years, and there is a male predominance [5]. Clinical symptoms of IgG4-RLD are nonspecific, and include cough, dyspnea, fever, and chest pain, but more than half of patients are without pulmonary symptoms [5]. Radiologic features of IgG4-RLD vary, and include ground-glass opacity, nonspecific interstitial pneumonia, organizing pneumonia, sclerosing mediastinitis, mediastinal or hilar adenopathy, airway stenosis, and pleural disease. Hilar and mediastinal adenopathy is the most common form. A combination of pulmonary abnormalities often present in the same patient [4-5]. All of these image patterns are related pathologically to lymphoplasmacytic infiltration with fibrosis. Proposed diagnostic criteria for IgG4-related respiratory disease suggest that specimens from intrathoracic tissues should meet 2 or more of the following criteria in the histology exam: (1) marked lymphoplasmacytic cell infiltration, (2) an IgG4/IgG-positive cell ratio 40% or higher and/or >10 IgG4-positive cells/HPF, (3) obliterative phlebitis or obliterative arteritis, and (4) storiform fibrosis or fibrosis consisting of proliferating spindle-shaped cells around infiltrating lymphocytes [6]. In the clinical exam, most patients with solid nodular or round-shaped ground-glass opacity in the lung and hilar lymphadenopathies are recognized as having lung cancer initially. The small size of the lung specimens from CT-guided biopsy or bronchoscopic biopsy is not adequate to reveal all of these histologic features. Biopsies of lymph nodes are difficult to interpret in the diagnosis of IgG4-RD because they seldom express the storiform fibrosis that is highly characteristic of an IgG4-RD diagnosis, and large numbers of IgG4+ plasma cells can be found in multiple diseases, such as hyper-interleukin-6 syndromes, Rosaii-Dorfman disease and granulomatosis with polyangiitis, in which IgG4-RD is not the diagnosis [5]. Patients with lung cancer complicated with IgG4-RLD have also been reported [7-8]. The possibility of the coexistence of IgG4-RLD and lung cancer should be kept in mind. Up to the present, surgical lung biopsy is the most important tool for the histological diagnosis of IgG4-RLD.

Serum IgG4 level is the most sensitive and specific laboratory test for the diagnosis of IgG4-RD. A serum IgG4 concentration greater than or equal to 135 mg/dL is considered clinically significant. Testing the serum IgG4 level in patients with complex radiologic findings, especially in multiple lobes, is recommended [9]. Tsushima *et al*. reported elevated serum IgG4 among patients with suspected sarcoidosis and higher levels of bronchoalveolar lavage (BAL) IgG4, IgG4/IgG, and IgG4/IgG3 [10]. BAL has played a role in the diagnosis of IgG4-RLD in a few reports [10-11].

No randomized trials regarding the treatment of IgG4-RD have been conducted. The international consensus guideline statement on the management and treatment of IgG4-RD [11] is based upon web-based questionnaires, face-to-face discussion and a literature review. Treatment for patients with symptomatic, active IgG4-RD is suggested. Glucocorticoids are first-line agents for induction therapy in all patients with active, untreated IgG4-RD. Patients

with multi-organ disease, significantly elevated serum IgG4 concentrations, involvement of the proximal bile ducts, or a history of disease relapse are at higher risk of early recurrence [12]. Patients with an organ-threatening IgG4-RD manifestation or with an elevated risk of relapse may benefit from maintenance therapy. Maintenance therapy may consist of low-dose glucocorticoids or other steroid-sparing agents. B-cell depletion with rituximab has also been useful as maintenance therapy. The optimal duration of maintenance therapy has not been established. Among 458 patients in a large autoimmune pancreatitis registry from Japan that received glucocorticoid maintenance therapy, 134 (29.6%) showed relapse on imaging studies [13]. A history of relapse appears to be a strong predictor of future relapse.

Cases with clinical and histopathological similarities between lupus nephritis and IgG4-related kidney disease have been reported [14-15]. To the best of our knowledge, this is the first report of a patient with IgG4-RLD and SLE simultaneously.

Identifying IgG4-RLD is clinically challenging. Surgical lung biopsy and serum IgG4 concentration measurement are important methods for diagnosis. Development of less invasive diagnostic tools and criteria with high accuracy in the future is important.

References

1. Hamano H, Kawa S, Horiuchi A, *et al*. High serum IgG4 concentrations in patients with sclerosing pancreatitis. N Engl J Med 2001; 344: 732-8.
2. Duvic C, Desrame J, Leveque C, *et al*. Retroperitoneal fibrosis, sclerosing pancreatitis and bronchiolitis obliterans with organizing pneumonia. Nephrol Dial Transplant 2004; 19: 2397-9.
3. Taniguchi T, Ko M, Seko S, *et al*. Interstitial pneumonia associated with autoimmune pancreatitis. Gut 2004 May; 53(5): 770-1.
4. Raj R. IgG4-related lung disease. Am J Respir Crit Care Med 2013 Sep 1; 188(5): 527-9.
5. Campbell SN, Rubio E, Loschner AL. Clinical review of pulmonary manifestations of IgG4-related disease. Ann Am Thorac Soc 2014 Nov; 11(9): 1466-75.
6. Matsui S, Yamamoto H, Minamoto S, *et al*. Proposed diagnostic criteria for IgG4-related respiratory disease. Respir Investig 2016 Mar; 54(2): 130-2.
7. Zen Y, Inoue D, Kitao A, *et al*. IgG4-related lung and pleural disease: a clinicopathologic study of 21 cases. Am J Surg Pathol 2009; 33: 1886-93.
8. Inoue T, Hayama M, Kobayashi S, *et al*. Lung cancer complicated with IgG4-related disease of the lung. Ann Thorac Cardiovasc Surg 2014; 20 Suppl: 474-7.
9. Inoue D, Zen Y, Abo H, *et al*. Immunoglobulin G4-related lung disease: CT findings with pathologic correlations. Radiology 2009 Apr; 251(1): 260-70.
10. Tsushima K, Yokoyama T, Kawa S, *et al*. Elevated IgG4 levels in patients demonstrating sarcoidosis-like radiologic findings. Medicine (Baltimore) 2011 May; 90(3): 194-200.
11. Tsushima K, Tanabe T, Yamamoto H, *et al*. Pulmonary involvement of autoimmune pancreatitis. Eur J Clin Invest 2009 Aug; 39(8): 714-22.
12. Khosroshahi A, Wallace ZS, Crowe JL, *et al*. International consensus guidance statement on the management and treatment of IgG4-related disease. Arthritis Rheumatol 2015 Jul; 67(7): 1688-99.
13. Kanno A, Nishimori I, Masamune A, *et al*. Research Committee on Intractable Diseases of Pancreas. Nationwide epidemiological survey of autoimmune pancreatitis in Japan. Pancreas 2012; 41: 835-9.
14. Yahata M, Takahashi S, Nakaya I, *et al*. Possible IgG4-related kidney disease requiring a differential diagnosis of membranous lupus nephritis. Intern Med 2012; 51(13): 1731-6.
15. Zaarour M, Weerasinghe C, Eter A, *et al*. An overlapping case of lupus nephritis and IgG4-related kidney disease. J Clin Med Res 2015 Jul; 7(7): 575-81.

IgG4 相關肺部疾病合併紅斑性狼瘡：病例報告

張立群　吳政翰 *　許嘉林　施金元　余忠仁

IgG4 相關肺部疾病是 IgG4 相關疾病的肺部表現，為一相當罕見的疾病，因常合併淋巴結病變，影像上不易與肺癌區分。本篇文章探討一位六十七歲、IgG4 相關肺部疾病合併紅斑性狼瘡的病人，一開始在健康檢查中發現肌酸酐上升、貧血、白血球低下與肺部腫塊，腹部磁振造影可見胰臟腫大及雙側腎臟病灶，經胸腔內視鏡影像輔助手術肺部切片證實為 IgG4 相關肺部疾病，胰臟腫大在治療後漸漸改善，血清 IgG4 濃度亦逐漸下降。當發現有肺腫瘤，懷疑為 IgG4 相關肺部疾病，血清 IgG4 濃度及胸腔內視鏡影像輔助手術肺部切片為疾病診斷的重要工具。*(胸腔醫學 **2018; 33: 70-75**)*

關鍵詞：IgG4 相關肺部疾病，紅斑性狼瘡

國立台灣大學醫學院附設醫院　內科部　胸腔科，* 國立台灣大學醫學院附設醫院　內科部　風濕免疫科
索取抽印本請聯絡：許嘉林醫師，國立臺灣大學醫學院附設醫院　內科部　胸腔科，台北市中山南路 7 號

Endobronchial Aspergilloma with Hemoptysis in an Immunocompetent Patient: A Case Report and Literature Review

Shih-Hsuan Peng, Sheng-Huei Wang, Chung-Kan Perng, Chih-Feng Giian, Wann-Cherng Perng, Chih-Hao Shen

Aspergillosis is associated with a variety of clinical infections in the thorax, and endobronchial aspergilloma is a rare presentation of pulmonary aspergillosis. Endobronchial aspergilloma may affect immunocompromised patients, but it is also found in immunocompetent patients. Herein, we describe the case of a 63-year-old woman without underlying disease who presented complaining of hemoptysis for 2 days. Chest computed tomography showed only an accumulation of fluid-like material at the bronchus of the right upper lobe. Persistent hemoptysis was apparent during the first 6 days of hospitalization. Flexible bronchoscopy revealed a ball-like mass of necrotic tissue that contained fungal hyphae as determined by histopathology, consistent with a diagnosis of endobronchial aspergilloma. The aspergilloma was removed and the patient's symptoms were relieved. This case highlights that endobronchial aspergilloma in immunocompetent patients may be associated with clinical pictures that differ from those of immunocompromised patients with endobronchial aspergilloma. Timely bronchoscopy to facilitate diagnosis is important for adequate management. ***(Thorac Med 2018; 33: 76-83)***

Key words: endobronchial aspergilloma, hemoptysis, immunocompetent

Introduction

Aspergillosis is the most common opportunistic mold infection worldwide, and is an important cause of mortality in patients with immune dysfunction [1]. *Aspergillus* spp. is present in the air and is easily inhaled by humans, being only approximately 2-3 μm in size. Most people inhale them every day without getting sick, but *Aspergillus* can cause disease in immunocompromised individuals or in those with severe lung damage. Many occupations, especially those involving outdoor activities, are associated with increased environmental exposure to *Aspergillus* and an increased risk of Aspergillosis. In addition, different lifestyle practices, such as smoking tobacco and pet ownership, may also lead to Aspergillosis in susceptible in-

Division of Pulmonary Medicine, Department of Internal Medicine, Tri-Service General Hospital, National Defense Medical Center, Taipei, Taiwan, Republic of China
Address reprint requests to: Dr. Chih-Hao Shen, Division of Pulmonary Medicine, Department of Internal Medicine, Tri-Service General Hospital, National Defense Medical Center, No. 325, Section 2, Cheng-Kung Road, Nei-Hu Dist. 114, Taipei, Taiwan, Republic of China

dividuals [2].

Thoracic involvement of *Aspergillus* is usually classified as allergic bronchopulmonary aspergillosis (ABPA), invasive pulmonary aspergillosis (IPA), chronic necrotizing pulmonary aspergillosis (CNPA), or aspergilloma [3-4]. ABPA is an allergic pulmonary disorder, manifesting mainly as asthma, and is related to the presence of *Aspergillus* antigens. IPA is characterized by tissue invasion and is usually observed in severely immunocompromised patients, while CNPA is usually associated with local pulmonary invasion in patients with chronic lung disease or diabetes mellitus, or in those on corticosteroid therapy or exhibiting malnutrition. Aspergilloma refers to a mass composed of a fungus ball containing fibrin, mycelia, septate hyphae, and blood cells that *Aspergillus* has colonized, which is incorporated into the pre-existing cavity [3-4]. Aspergilloma in the thorax can be classified into 3 types: pulmonary aspergilloma, pleural aspergilloma, and endobronchial aspergilloma [5]. Pulmonary aspergilloma usually grows into the pre-existing lung cavity from the residue of pulmonary tuberculosis (TB), sarcoidosis, or pneumoconiosis [6-7]. Most cases of pulmonary aspergilloma involve a thin-walled cavity with little or no surrounding parenchymal disease, and usually the patient has few symptoms and exhibits little evidence of systemic inflammation [8]. Pleural aspergilloma is usually found after chronic empyema or surgical complications, where the suppuration produces an environment conducive to colonization by *Aspergillus* [9].

Endobronchial aspergilloma is a rare presentation of pulmonary aspergillosis, and a rare cause of endobronchial mass. It is characterized by the growth of *Aspergillus* into the bronchial lumen. The diagnosis of endobronchial aspergilloma is based on the presence of an intraluminal mass or necrotic tissue on bronchoscopy, and separated fungal hyphae with acute branching angles characteristic of *Aspergillus* species on histological examination. The first report of endobronchial aspergilloma involved a patient with human immunodeficiency virus (HIV) [10]. However, endobronchial aspergilloma has also been reported in immunocompetent patients [11-13]. Herein, we describe the case of an immunocompetent patient with endobronchial aspergilloma presenting with recurrent hemoptysis.

Case Report

A 63-year-old woman was admitted with a 2-day history of intermittent chest tightness and cough with blood-tinged sputum. The quantity of blood from hemoptysis was approximately 100 ml per day. She had also suffered from progressive cough and shortness of breath during the previous 1 year. She had never smoked, and had suffered from pulmonary TB during childhood that had been fully treated. She did not have diabetes, cirrhosis, chronic kidney disease, cancer, hematologic disease, or any rheumatic disease, and had not taken corticosteroids or other immunosuppressive medication. The patient was a homemaker with no current involvement in outdoor activities, and was not a pet owner.

On admission, she presented with blood pressure of 118/68 mmHg, a heart rate of 72 beats per minutes, a respiration rate of 18 breaths per minute, and body temperature of 36.8°C. Auscultation of the chest revealed expiratory wheezing in the right upper lung, and rhonchi in the right lung fields. Complete blood count results were white blood cells 12,610/

mm^3 (neutrophils 77.6%, lymphocytes 19.5%, monocytes 2.5%, and eosinophils 0.5%), hemoglobin 11.7 g/dl, and platelets 221,000/mm^3. Coagulation tests including prothrombin time, international normalized ratio, and partial thromboplastin time were all within normal limits. Chest x-ray showed small granulomas in the right middle lung field (Figure 1). Panendoscopy was performed based on a suspicion of hematemesis, but showed only gastroesophageal reflux without evidence of recent bleeding. Chest computed tomography revealed cystic bronchiectasis in the right upper lobe, cylindrical bronchiectasis in the right middle lobe filled with fluid-like material, and bilateral traction bronchiectasis of the lower lobes (Figure 2). The patient underwent bronchoscopy in the poor visual fields on the second day of hospitalization for hemoptysis, but this revealed only substantial blood clotting at the left and right main bronchus. Interventions including fluid resuscitation, blood transfusion, and intravenous hemostatic medications were administered.

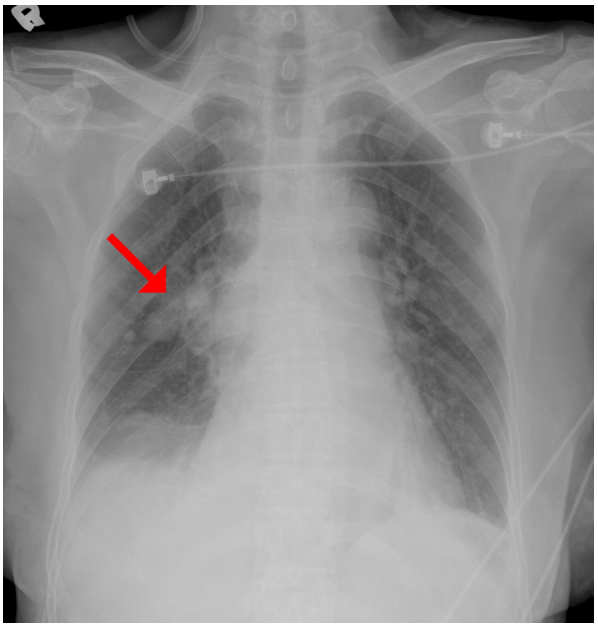

Fig. 1. Chest radiography revealed small granulomas in the right middle lung field.

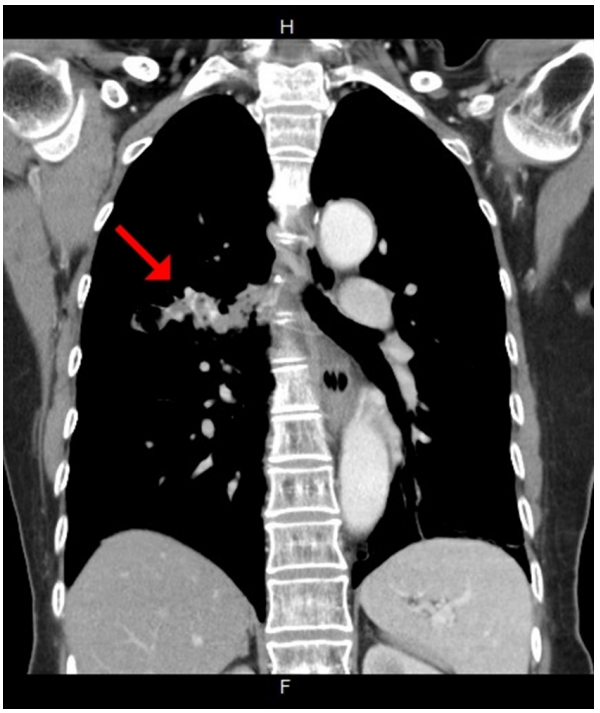

Fig. 2. Chest computed tomography showed fluid-like material accumulation in the right middle lobe.

A secondary bronchoscopy was performed on the sixth day of hospitalization, and revealed a brownish, movable, ball-like mass of necrotic tissue in the posterior branch of the right upper lobe bronchus (RB2), associated with hyperemia of the bronchial wall (Figure 3A); the whole lesion was removed via fixed bronchoscopy. Histopathological analysis revealed a sphere of necrotic tissue containing fungal hyphae with acute branching angles of approximately 45 degrees, and frequent septa of the pulmonary tissue (Figure 3B), characteristic of aspergilloma. During hospitalization, all sputum cultures, sputum acid-fast bacilli smears, TB polymerase chain reaction, and HIV antibody tests were negative. Tumor markers including carcinoembryonic antigen and squamous cell

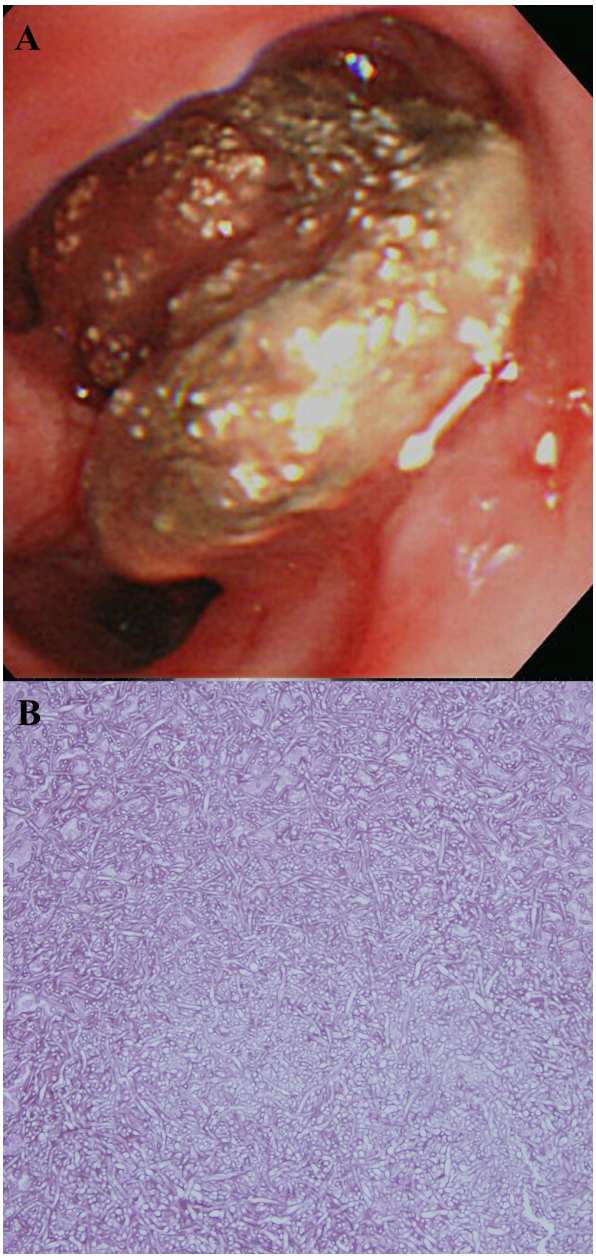

Fig. 3. (A) Bronchoscopy revealed a brownish, movable, ball-like mass in the RB2 bronchus. (B) The histological picture showed fungal hyphae in the mass.

carcinoma antigen were within normal range. After removal of the fungal ball, the patient's shortness of breath and hemoptysis gradually subsided and no medications were needed for subsequent management. Granulomas in the right middle lung field had diminished in a subsequent chest x-ray (Figure 4). The patient was discharged with complete remission of symptoms 10 days after initial hospitalization. She reported no recurrence of disease at a 6-month follow-up examination.

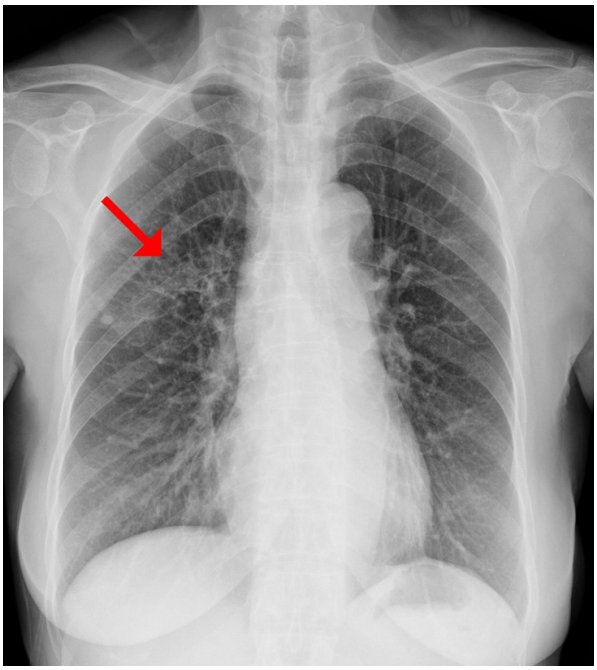

Fig. 4. Follow-up chest radiography revealed diminished granulomas in the right middle lung field.

Discussion

We described a rare case of endobronchial aspergilloma initially associated with hemoptysis. After removal of the lesion, no further invasiveness was observed at follow-up. Endobronchial aspergilloma is usually detected incidentally, while investigating the cause of hemoptysis, bronchial obstruction, or parenchymal lung lesion via bronchoscopy [1], and the current case is the first reported in Taiwan.

In addition to the present case, we identified 19 other cases of endobronchial aspergilloma

Table 1. Review of Endobronchial Aspergilloma

Reference	Age/ Sex	Hemoptysis	Smoking	Pulmonary TB	Lung cancer	Immunocompromised status	Location	Medical Treatment	Follow-up
Argento AC, *et al*. (15)	63/M	No	NA	None	None	Chronic lymphoid leukemia	Subglottic trachea	Voriconazole, Micafungin, Amphotericin B	Expired
Argento AC, *et al*. (15)	52/M	No	NA	None	None	Acquired immune deficiency syndrome	Main carina	Voriconazole, Micafungin	Fistula and stenosis of the bronchus
Araújo D, *et al*. (16)	64/M	No	NA	Active pulmonary TB	None	Rheumatoid arthritis	Lingular division of left upper lobe	Voriconazole	Expired
Argento AC, *et al*. (15)	68/M	No	NA	None	None	Post-heart transplantation	Distal tracheal/ right mainstem bronchus	Voriconazole, Micafungin, Amphotericin B	Tracheal fistula
Sunnetcioglu A, *et al*. (17)	28/M	Yes	NA	None	None	Acute lymphoblastic leukemia	Entrances of right middle lobe	Voriconazole	No complication
Ma JE, *et al*. (12)	50/M	Yes	Current smoker	None	Non-small cell lung cancer	None	Superior segment of left lower lobe	None	No complication
Ma JE, *et al*. (12)	70/M	No	Current smoker	Active pulmonary TB	Non-small cell lung cancer	None	Anastomosis site of right upper lobe	Itraconazole	No complication
Shenghua J, *et al*. (14)	56/F	Yes	NA	None	Bronchopulmonary neuroendocrine carcinoma	None	Lingular division of left upper lobe	Voriconazole, Caspofungin	No complication
Shenghua J, *et al*. (14)	50/F	Yes	NA	None	Adenocarcinoma	None	Right lower lobe	Itraconazole	No complication
Ma JE, *et al*. (12)	70/M	Yes	Current smoker	Old pulmonary TB	None	None	Apical segment of left upper lobe	None	No complication
Ma JE, *et al*. (12)	51/M	Yes	Non-smoker	Old pulmonary TB	None	None	Apical segment of left upper lobe	None	No complication
Ma JE, *et al*. (12)	46/M	Yes	Current smoker	Old pulmonary TB	None	None	Apicoposterior segment of left upper lobe	None	No complication
Ma JE, *et al*. (12)	76/M	No	Ex-smoker	Old pulmonary TB	None	None	Apicoposterior segment of left upper lobe	None	No complication
Ma JE, *et al*. (12)	36/M	Yes	Ex-smoker	Old pulmonary TB	None	None	Left upper lobe	None	No complication
Kim SJ, *et al*. (11)	33/M	Yes	NA	None	None	None	Laterobasal segment of left lower lobe	None	No complication
Ma JE, *et al*. (12)	75/M	No	Ex-smoker	None	None	None	Apicoposterior segment of left upper lobe	Itraconazole	No complication
Ma JE, *et al*. (12)	53/F	No	Non-smoker	None	None	None	Apical segment of right upper lobe	None	No complication
Ma JE, *et al*. (12)	57/M	No	Non-smoker	Old pulmonary TB	None	None	Lingular division of left upper lobe	None	No complication
Junge SW, *et al*. (13)	59/M	Yes	NA	None	None	None	Superior segment of left lower lobe	None	No complication
The present case	63/F	Yes	Non-smoker	Old pulmonary TB	None	None	Posterior segment of right upper lobe	None	No complication

in a PubMed search of the literature [11-17] (Table 1). Of the 20 total patients, most (16/20) were male. The mean age was 56 years (range 28-76 years). Five were classified as immunocompromised, including patients with chronic lymphoid leukemia, acute lymphoblastic leukemia, HIV, and immunosuppressive therapy for rheumatoid arthritis and heart transplantation [15-17]. Four patients had had pre-existing lung cancer with treatment [12,14], and the other 11 were immunocompetent. Symptoms and clinical courses varied between the immunocompromised and immunocompetent patients, and may also vary between immunocompetent patients themselves.

The current patient had a history of childhood pulmonary TB. This prior exposure to TB, a risk factor for pulmonary aspergilloma, was also reported in 9 of the patients identified in our literature review. Of these, 2 patients (1 with an immunocompromised status, and 1 with lung cancer) suffered from active pulmonary TB [12,16]. Hemoptysis may be caused by vascular damage via local invasion of adjacent vessels, mechanical effects of a fungus ball, or fungal toxins [5]. In our review, hemoptysis was present in 10 patients, and the incidence of hemoptysis was higher in immunocompetent than in immunocompromised patients. Conversely, in immunocompromised patients, cough, dyspnea, and other non-specific symptoms were more common.

In our review, most of the patients with endobronchial aspergilloma exhibited it in the upper lobe and lower lobe superior segment (14/20). Only 3 patients had endobronchial aspergilloma located in the trachea or carina, and all 3 were immunocompromised. Since pulmonary aspergilloma is also mainly found in the upper lobe and lower lobe superior segment, these findings suggest that these 2 locations present a nidus or structural change that can result in an airflow stasis for the colonization of *Aspergillus* in the bronchial lumen [4,18].

Without treatment, some patients with pulmonary aspergilloma may remain stable over long periods, regress, and even spontaneously resolve [5]. Removal of aspergilloma via scope forceps or a surgical approach may be considered in patients with pulmonary aspergilloma and severe hemoptysis [19-20]. There is no consensus in the literature regarding the management of endobronchial aspergilloma. In our review, the endobronchial aspergilloma was removed in all reported cases. In addition, antifungal regimens were used in 9 patients. Most of these (8/9) had an immunocompromised status or had lung cancer. With regard to immunocompetent patients, most (10/11) did not receive anti-fungal treatment and there were no complications noted in follow-up examinations. However, immunocompromised patients and those with lung cancer who received antifungal regimens were more likely to develop complications in follow-up examinations, and mortality was more likely.

In conclusion, endobronchial aspergilloma is an unusual cause of hemoptysis. Patients with endobronchial aspergilloma may exhibit differences in clinical imaging and prognoses, depending on whether they are immunocompromised or immunocompetent. Timely bronchoscopy to facilitate an accurate diagnosis is important for adequate management.

References

1. Mehrad B, Paciocco G, Martinez FJ, *et al*. Spectrum of Aspergillus infection in lung transplant recipients: case series and review of the literature. Chest 2001; 119: 169-

75.
2. Sipsas NV, Kontoyiannis DP. Occupation, lifestyle, diet, and invasive fungal infections. Infection 2008; 36: 515-25.
3. Soubani AO, Chandrasekar PH. The clinical spectrum of pulmonary aspergillosis. Chest 2002; 121: 1988-99.
4. Garnacho-Montero J, Olaechea P, Alvarez-Lerma F, *et al*. Epidemiology, diagnosis and treatment of fungal respiratory infections in the critically ill patient. Rev Esp Quimioter 2013; 26: 173-88.
5. Moodley L, Pillay J, Dheda K. Aspergilloma and the surgeon. J Thorac Dis 2014; 6: 202-9.
6. Franquet T, Muller NL, Gimenez A, *et al*. Spectrum of pulmonary aspergillosis: histologic, clinical, and radiologic findings. Radiographics 2001; 21: 825-37.
7. Park Y, Kim TS, Yi CA, *et al*. Pulmonary cavitary mass containing a mural nodule: differential diagnosis between intracavitary aspergilloma and cavitating lung cancer on contrast-enhanced computed tomography. Clin Radiol 2007; 62: 227-32.
8. Riscili BP, Wood KL. Noninvasive pulmonary Aspergillus infections. Clin Chest Med 2009; 30: 315-35.
9. Guazzelli LS, Severo CB, Hoff LS, *et al*. Aspergillus fumigatus fungus ball in the pleural cavity. J Bras Pneumol. 2012; 38: 125-32.
10. Denning DW. Commentary: unusual manifestations of aspergillosis. Thorax 1995; 50: 812-3.
11. Kim JS, Rhee Y, Kang SM, *et al*. A case of endobronchial aspergilloma. Yonsei Med J 2000; 41: 422-5.
12. Ma JE, Yun EY, Kim YE, *et al*. Endobronchial aspergilloma: a report of 10 cases and literature review. Yonsei Med J 2011; 52: 787-92.
13. Jung SW, Kim MW, Cho SK, *et al*. A case of endobronchial aspergilloma associated with foreign body in immunocompetent patient without underlying lung disease. Tuberc Respir Dis (Seoul) 2013; 74: 231-4.
14. Jiang S, Jiang L, Shan F, *et al*. Two cases of endobronchial aspergilloma with lung cancer: a review of the literature of endobronchial aspergilloma with underlying malignant lesions of the lung. Int J Clin Exp Med 2015; 8: 17015-21.
15. Argento AC, Wolfe CR, Wahidi MM, *et al*. Broncho-mediastinal fistula caused by endobronchial aspergilloma. Ann Am Thorac Soc 2015; 12: 91-5.
16. Araújo D, Figueiredo M, Monteiro P. Endobronchial aspergilloma: An unusual presentation of pulmonary aspergillosis. Rev Port Pneumol (2006) 2016; 22: 61-2.
17. Sunnetcioglu A, Ekin S, Erten R, *et al*. Endobronchial aspergilloma: A case report. Respir Med Case Rep 2016; 18: 1-3.
18. Belcher JR, Plummer NS. Surgery in broncho-pulmonary aspergillosis. Br J Dis Chest. 1960; 54: 335-6.
19. Andersen PE. Imaging and interventional radiological treatment of hemoptysis. Acta Radiol 2006; 47: 780-92.
20. Lejay A, Falcoz PE, Santelmo N, *et al*. Surgery for aspergilloma: time trend towards improved results? Interact Cardiovasc Thorac Surg 2011; 13: 392-5.

支氣管內麴菌球合併咳血於免疫健全患者：病例報告與文獻回顧

彭士軒　王勝輝　彭忠衍　簡志峰　彭萬誠　沈志浩

麴菌在胸腔內有許多不同的臨床形式，而支氣管內麴菌球則是少見的肺麴菌病表現。支氣管內麴菌球通常是影響免疫不全的病患，但也會在免疫健全的病患中發現。我們的案例報告是一位沒有潛在疾病的63歲女性，主訴咳血2天。胸部電腦斷層只發現有液體狀的物質堆積在右上葉支氣管內。但是咳血仍然在住院的前6天持續出現。支氣管鏡檢查則發現一顆包含壞死組織的球狀腫塊，這個腫塊的病理報告顯示內含真菌菌絲，因此診斷為支氣管內麴菌球。病患的症狀在此麴菌球被移除後也就逐漸緩減。這個病例說明免疫健全的病患感染支氣管內麴菌球時可能會和免疫不全的病患有不同的臨床表現。及時的支氣管鏡檢查對於診斷及適當的治療是很重要的。*(胸腔醫學* ***2018; 33: 76-83)***

關鍵詞：支氣管內麴菌球，咳血，免疫健全

三軍總醫院　內科部　胸腔內科
索取抽印本請聯絡：沈志浩醫師，三軍總醫院　內科部　胸腔內科，台北市內湖區成功路二段325號

Carcinoid Tumor in Intralobar Pulmonary Sequestration: A Case Report

Hsin-Yueh Fang, Yi-Cheng Wu, Yun-Hen Liu, Ming-Ju Hsieh, Yin-Kai Chao, Ching-Yang Wu, Wei-Hsun Chen

Pulmonary sequestration is a congenital abnormality characterized by abnormal bronchial development and a lack of connection of a systemic arterial blood supply. We present the case of a 57-year-old male with the symptom of hemoptysis, who underwent surgical resection of the left lower lobe. However, the final histological pathology revealed a carcinoid tumor in the pulmonary sequestration. Although the exact pathway leading to the development of carcinoma is still unknown, a malignant degeneration must also be considered in lung sequestration. ***(Thorac Med 2018; 33: 84-88)***

Key words: pulmonary sequestration; carcinoid tumor; cancer; hemoptysis

Introduction

Pulmonary sequestration is a congenital abnormality characterized by abnormal bronchial development without communication with bronchial trees and without a systemic arterial blood supply. We present the case of a patient with the symptom of refractory hemoptysis, who underwent surgical resection of the left lower lobe (LLL). The final pathological examination revealed a carcinoid tumor in the pulmonary sequestration.

Case Report

A 57-year-old male worked as a plumber and was a heavy smoker for 30 years. He denied any history of systemic disease. He complained of hemoptysis for 10 days, with blood clots in the sputum. The patient denied cough, shortness of breath, chest tightness, and fever during this period. Physical examination showed no obvious abnormality except crackles in the LLL area. The biochemistry examination reported leukocytosis. Chest x-ray revealed mildly increased infiltration in the LLL area (Figure 1). The patient initially was treated with the antibiotics ciprofloxacin and metronidazole for LLL pneumonia. However, after a 1-week treatment course, the patient still complained of intermittent hemoptysis. Computed tomography (CT) of the artery was performed, and showed pulmonary embolus at the left inferior pulmonary artery and LLL pulmonary sequestration

Division of Thoracic and Cardiovascular Surgery, Chang Gung Memorial Hospital, Chang Gung University, Taoyuan, Taiwan
Address reprint requests to: Dr. Hsin-Yueh Fang, Division of Thoracic & Cardiovascular Surgery, Chang Gung Memorial Hospital, 5 Fu-Hsing St, Kwei-Shan, Taoyuan, Taiwan 33305

Fig. 1. CXR show increased infiltration in the left lower lung

with a feeding vessel from the thoracic aorta (Figure 2). However, the patient did not receive anticoagulation therapy for the pulmonary embolus because of persistent hemoptysis. Due to the persistent symptoms, the patient requested surgical treatment.

During operation, a feeding vessel from the thoracic aorta at the supra-diaphragm level to the LLL intralobar pulmonary sequestration was found and resected, and then LLL lobectomy was performed. LLL consolidation with a great deal of hematoma was found in the specimen grossly. Final pathology reported a solid mass, 2.7cm in diameter, which was revealed to be typical carcinoid tumor with uniform cells in an organoid pattern without mitosis or necrosis. The immunohistochemical study results were positive for cd56 (1B6), chromogranin a (DAK-A3) and synaptophysin (SY-38); a typical carcinoid tumor therefore was diagnosed. The patient recovered smoothly and was discharged 1 week after surgery, with no more hemoptysis. No distant metastasis was found on the positron emission tomography (PET) scan 2 months after operation. The patient was followed-up regularly with chest CT every 6 months; no tumor recurrence or distal metastasis was found.

Discussion

Pulmonary sequestration is a congenital ab-

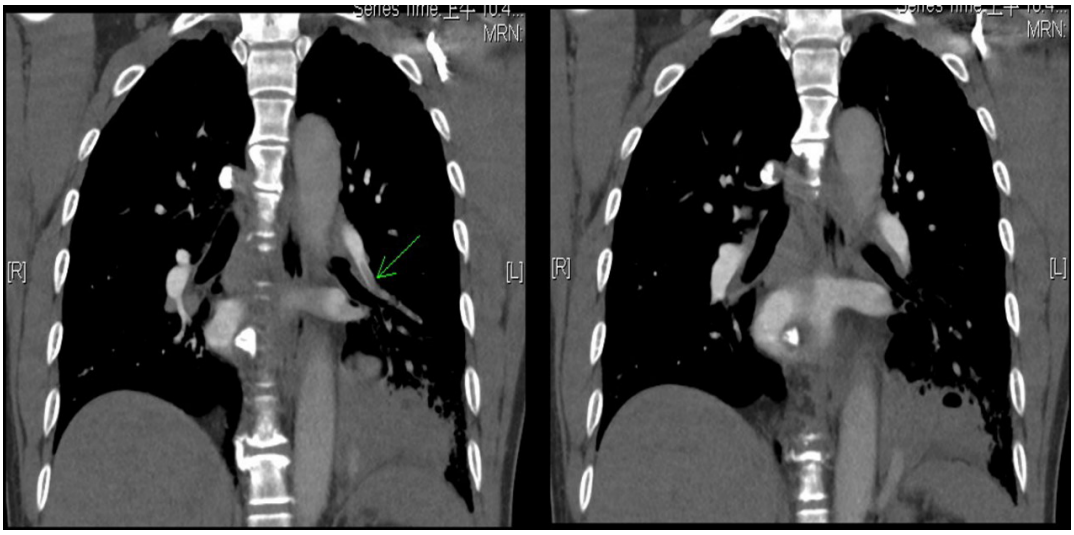

Fig. 2. Pulmonary embolus at the left inferior pulmonary artery (left) and left lower lobe pulmonary sequestration with a feeding vessel from the thoracic aorta (right)

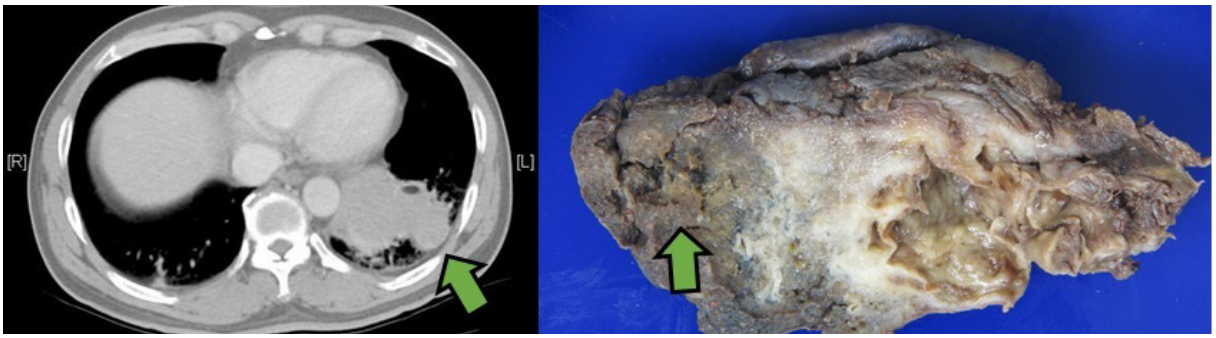

Fig. 3. A mass-like lesion at the peripheral side of the lung sequestration. Chest-abdominal view (left) and a picture of the gross specimen (right). The green arrow indicates the possible tumor location within the pulmonary sequestration.

normality characterized by abnormal bronchial development without communication with the bronchial trees and without a systemic arterial blood supply. The most common symptom is recurrent infection, but fatal hemoptysis has also been described [1]. Pulmonary sequestration can be divided into 2 subgroups based on the anatomy: intralobar sequestration (ILS), which frequently shows signs of respiratory tract infection, and extralobar sequestration (ELS), which is generally asymptomatic [2].

Pulmonary carcinoid tumors originate from endocrine tumors, and account for about 25-30% of all carcinoid tumors and about 3% of all pulmonary tumors [3]. In the 2004 World Health Organization (WHO) classification, pulmonary carcinoid tumors are divided into 4 major types: typical carcinoid (2%), atypical carcinoid (0.2%), large-cell neuroendocrine carcinoma (3%), and small-cell lung cancer (20%).

There are only a few case reports on malignant neoplasms in intrapulmonary sequestration. The most common diagnosis is squamous cell carcinoma, followed by adenocarcinoma and carcinoid tumor [4]. The symptoms differ among cases, but hemoptysis and recurrent pneumonia are the most common in pulmonary sequestration, and thus most of the neoplasms are diagnosed incidentally after resection. In our case, the pre-operative image could not distinguish the tumor location exactly before operation, because the lesion was located in the sequestration parenchyma. When we reviewed the image, the tumor-like lesion appeared to be located on the peripheral side of the sequestration (Figure 3). Belchis *et al* mentioned 3 possible pathways leading to malignant transformation [5]: first, the tumor may progress from an underlying cancer predisposition syndrome, such as a premalignant cystic lesion, to a sarcoma; second, there may be an innate propensity to undergo malignant degeneration in the mucinous cells; and third, a malignant formation may result from frequent chronic inflammation. However, the exact pathway leading to the development of malignancy is still unknown. Since the tumor was found accidently, lymph node dissection was not performed during operation. Therefore, a complete post-operative study for tumor staging was important. We performed a PET scan for the patient about 2 months after operation, and no distant metastasis was seen. The patient underwent chest CT every 6 months thereafter, and no distant metastasis was found.

In our literature review, we found that this

was the first reported case of carcinoid tumor in intralobar pulmonary sequestration in Taiwan. Pulmonary sequestration is usually diagnosed via imaging when symptoms are refractory to conservative therapy, and surgical intervention is the main mode of treatment [1]. However, a patient may be treated with medication for a long time without worsening symptoms, even if there is a neoplasm in the sequestration that, may progress during this period and may involve other organ in the future. Thus, a patient with pulmonary sequestration should receive regular follow-up examination, and clinicians should always consider the possibility of tumor formation in this group.

References

1. Nowak K, von der Thüsen J, Karenovics W, *et al*. Pulmonary sequestration with haemoptysis and an unsuspected carcinoid tumour. Gen Thorac Cardiovasc Surg 2013; 61: 479-82.
2. Dae S, Sun A, Hyeong R, *et al*. Bronchial carcinoid tumor arising from an intralobar bronchopulmonary sequestration. Korean J Thorac Cardiovasc Surg 2011; 44: 444-7.
3. Burcharth F, Axelsson C. Lung carcinoids. Scand J Thorac Cardiovasc Surg 1973; 7: 72-7.
4. Sato S, Kitahara A, Koike T, *et al*. A case of ectopic ACTH-producing pulmonary carcinoid arising in an extralobar pulmonary sequestration. Int J Surg Pathol 2016; 24(2): 130-4.
5. Belchis D, Cowan M, Mortman K, *et al*. Adenocarcinoma arising in an extralobar sequestration: a case report and review of the literature. Lung Cancer 2014; 84: 92-5.

在隔離肺中診斷之肺部類癌：病例報告

范馨月　吳怡成　劉永恆　謝明儒　趙盈凱　吳青陽　陳維勳

隔離肺是一種先天性的肺部結構異常，主要表現為異常結構的支氣管分布及系統性的血管供應。本文提出一位 57 歲男性病患，因藥物無法治癒之咳血症狀，接受左下葉及隔離肺之切除，在病理報告中診斷出肺部類癌。雖然確切癌化的致病機轉上不明確，對於有症狀之隔離肺病患，癌變的診斷應被納入考慮。*(胸腔醫學* ***2018; 33: 84-88****)*

關鍵詞：隔離肺，類癌，腫瘤，咳血

長庚紀念醫院　胸腔及心臟血管外科
索取抽印本請聯絡：范馨月醫師，長庚紀念醫院　胸腔及心臟血管外科，33305 桃園市龜山區復興街 5 號

Successful Management with Hyperbaric Oxygen Therapy in Computed Tomography-Guided Core Needle Biopsy of the Lung Complicated with Air Embolism

Wei-Ting Chen, Chiung-Zuei Chen

Computed tomography-guided lung biopsy is a widely accepted and frequently performed procedure for pulmonary lesions; however, it is associated with various complications including pneumothorax, hemoptysis and parenchymal hemorrhage. Mild, self-limiting pneumothorax and hemoptysis are common complications of this procedure. Air embolism is a potentially life-threatening but extremely rare complication. We report a case of air embolism in the ascending aorta that developed during a computed tomography-guided percutaneous needle biopsy of the lung. The air embolism resolved uneventfully after a 1-hour hyperbaric oxygen therapy treatment session. No cardiac or cerebral symptoms were seen after this treatment. ***(Thorac Med 2018; 33: 89-94)***

Key words: CT-guided transthoracic lung biopsy, Air embolism

Introduction

Computed tomography (CT)-guided percutaneous core needle biopsies of lung lesions are often performed and are generally regarded as safe procedures with limited morbidity and extremely rare mortality. The most common complications are pneumothoax (27%), pulmonary hemorrhage (11%) and hemoptysis (7%) [1-3], all of which are usually conservatively treated and self-resolving. Severe complications such as tumor seeding through the biopsy track, tension pneumothorax, pulmonary hemorrhage and systemic air embolism are rare [3-9]. Air embolism is an extremely rare complication of CT-guided transthoracic biopsy. When air embolism occurs, it may be potentially life-threatening [4,6,9-10]. In most cases, management involves placing the patient in the Trendelenburg position to prevent embolization of the air into the cerebral circulation; 100% oxygen should be administered immediately and early hyperbaric oxygen (HBO) therapy is recommended [5,9]. Those managements promote the exchange of oxygen for nitrogen within the air bubbles and accelerate their resorption. Other supportive therapy such as anticonvulsant medication or steroids can be administered, and is indicated

Department of Internal Medicine, National Cheng Kung University College of Medicine and Hospital, Tainan, Taiwan
Address reprint requests to: Dr. Chiung-Zuei Chen, Department of Internal Medicine, National Cheng Kung University College of Medicine and Hospital, Tainan, Taiwan, No. 138, Sheng Li Road, Tainan, Taiwan 704, R.O.C

for cerebral air embolism if neurologic symptoms are present [4].

Case Report

A 44-year-old male patient had underlying systemic hypertension and a 20-year history of smoking and alcoholism. He had suffered from chest dullness for about 1 month. The pain was located at the anterior chest and occurred persistently every day in July, 2008. It was not effort-related and was not accompanied by cold sweating, and there were no apparent predisposing factors. He also complained of epigastric pain and acid regurgitation during the same period. Because of the above symptoms, he was referred to a GI specialist for suspected gastroesophageal reflux disease (GERD), which was confirmed by endoscopic examination later.

His epigastric pain improved after treatment for GERD, but his chest pain became bilateral at the T4 level, with a sharp pain radiating to the back that was worsened by changing positions and inspiration. He also had new symptoms, including productive cough with blood-tinged sputum and severe sharp pain in his left arm that was aggravated by motion of the left upper extremity weeks after follow-up at our OPD. Since his anterior chest pain and left arm pain were progressive and intolerable, a chest roentgenogram was taken and a left upper lung (LUL) mass was noted. CT study revealed a 4 x 4-cm cavitary mass in the LUL (Figures 1 and 2), a 1.9-cm nodule at the right adrenal gland and an osteolytic lesion at the left proximal humerus. He was then hospitalized for further survey in August, 2008.

During hospitalization, no other respiratory or constitutional symptoms were observed. General and systemic examinations were unremarkable. Routine blood examination was also normal. Mild hypercalcemia (10.3 mg/dL) and elevated CA199 (666.1 U/ml), a tumor marker, were noted. CT-guided transthoracic biopsy was arranged and performed on 15 August, 2008, and an air embolism was found (Figure 3). The patient's vital signs were stable, and no chest pains, palpitations or neurological defects were noted after the procedure on the table in the CT room. The patient was then placed in a totally supine position and maintained this position for

Fig. 1. A left upper lobe lung mass was noted by chest roentgenogram.

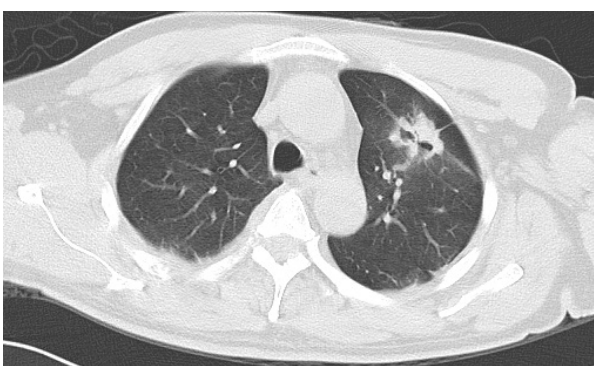

Fig. 2. CT scan of thorax reveals a 4 x 4 cm mass with cavitation and pleural tethering in the left upper lobe.

Fig. 3. CT scan of thorax showing biopsy needle inside the mass and intra-luminal air in ascending aorta was noted during the procedure.

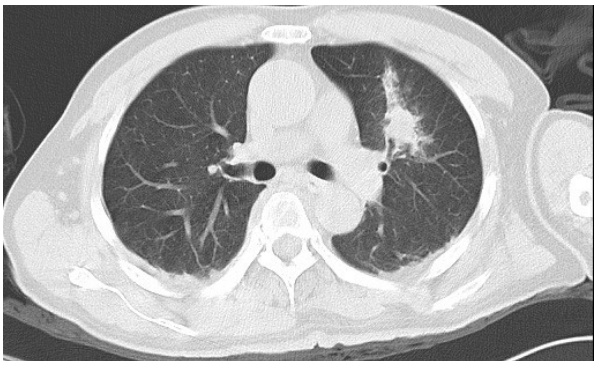

Fig. 4. CT scan of thorax showing no remaining air emboli were founded after 1 hour's HBO therapy

at least 48 hrs after the procedure, as ordered by the radiologist. To accelerate the patient's resolution of the air embolism, HBO therapy was arranged and performed soon after by his attending physician. After a 1-hour session of HBO therapy, no residual air emboli were found in the follow-up brain and chest CT (Figure 4). This patient was able to move freely and felt no discomfort after HBO therapy, and was thus discharged in a stable condition soon after the therapy.

Discussion

Severe complications such as systemic air embolism are rare [3-9]. However, the incidence rate of air embolism is believed to have been underestimated due to undiagnosed asymptomatic cases. Single-institutional, retrospective, observational studies based on the evaluation of CT scan images have suggested a higher incidence [5,7,9]. Hiraki *et al*. [5] found an incidence rate of 0.4%, with 4 cases of air embolism among 1,010 CT-guided lung biopsies, based on post-procedural CT scans of the entire thorax. Ibukuro *et al*. [7] estimated an incidence rate of 0.21%, based on a retrospective review of 1,400 cases of CT-guided lung biopsy. Freund *et al*. [8] reported that the radiological incidence of systemic air embolism complicating percutaneous core needle biopsy was 3.8%, whereas the clinically apparent incidence was 0.49%. This finding indicates that asymptomatic cases can lead to an overall under-diagnosis of this complication. Despite this higher radiological incidence rate, however, air embolism remains a relatively rare occurrence.

CT-guided transthoracic lung biopsies cause fewer systemic air embolisms than cardiac surgery, percutaneous coronary angiography, neurosurgical procedures in an upright position and barotrauma secondary to positive-pressure ventilation [9]. Mansour *et al*. listed 3 ways that air may enter the systemic circulation during the procedure [10]. The first is when the needle tip is placed within the pulmonary vein and the stylet has been removed, and communication between the atmosphere and pulmonary vein can occur. The second is when broncho-venous fistula are created as the needle passes through the lung parenchyma. In this situation, there may be communication between intra-alveolar

or intrabronchial air and the pulmonary vein due to elevated airway pressure. The third is that after traversing the pulmonary microvasculature, air in the pulmonary arterial circulation may reach the pulmonary venous circulation. With regard to our patient, the air might have entered the pulmonary vein via bronchoveneous fistula after the needle passed through the lung parenchyma, and eventually reached the ascending aorta through the circulation passing through the left atrium and ventricle.

Several precautionary methods have been designed to minimize the risk of developing this potentially fatal complication. For example, patients are told to hold their breath when instructed and avoid coughing during the procedure. The needle should also be inserted as rapidly as possible to prevent inadvertent ingress of air when the needle is open to the atmosphere. The opening should then be closed immediately using the operator's finger or a biopsy needle.

Conservative therapy consisting of inhalation of an atmosphere consisting of 100% oxygen resulted in significant improvement within 4 hrs in an asymptomatic patient [5]. Hyperbaric therapy is another treatment that can be used for air emboli. The volume of gas in an enclosed space is inversely proportional to the pressure exerted on it, and HBO therapy reduces the size of air bubbles and accelerates the dissolution of nitrogen by replacing nitrogen with oxygen [9].

We should keep in mind that this complication may occur even when excellent techniques are used with a cooperative patient by an experienced, skillful operator. Awareness of this complication cannot be overemphasized; clinicians should also be aware of the possible presence of systemic air and should be familiar with management techniques for dealing with this eventuality.

Conclusion

Air embolism is an extremely rare complication of CT-guided transthoracic biopsy. If air embolism occurs, place the patient in the Trendelenburg position to prevent the entrance of air embolization into the cerebral circulation; the immediate administration of 100% oxygen and early HBO therapy are also helpful.

References

1. Sinner WN. Complications of percutaneous transthoracic needle aspiration biopsy. Acta Radiol Diagn (Stockh) 1976; 17: 813-28.
2. Richardson CM, Pointon KS, Manhire AR, *et al*. Percutaneous lung biopsies: a survey of UK practice based on 5444 biopsies. Br J Radiol 2002; 75: 731-5.
3. Tomiyama N, Yasuhara Y, Nakajima Y, *et al*. CT-guided needle biopsy of lung lesions: a survey of severe complications based on 9783 biopsies in Japan. Eur J Radiol 2006; 59: 60-4.
4. Ohashi S, Endoh H, Honda T, *et al*. Cerebral air embolism complicating percutaneous thin-needle biopsy of the lung: complete neurological recovery after hyperbaric oxygen therapy. J Anesth 2001; 15: 233-6.
5. Hiraki T, Fujiwara H, Sakurai J, *et al*. Nonfatal systemic air embolism complicating percutaneous CT-guided transthoracic needle biopsy: four cases from a single institution. Chest 2007; 132: 684-90.
6. Ghafoori M, Varedi P. Systemic air embolism after percutaneous transthorasic needle biopsy of the lung. Emerg Radiol 2008; 15: 353-6.
7. Ibukuro K, Tanaka R, Takeguchi T, *et al*. Air embolism and needle track implantation complicating CT guided percutaneous thoracic biopsy: Single-institution experience. AJR Am J Roentgenol 2009; 193: W430-6.
8. Freund MC, Petersen J, Goder KC, *et al*. Systemic air embolism during percutaneous core needle biopsy of the lung: Frequency and risk factors. BMC Pulm Med 2012; 12: 2.

9. Peirce EC. Cerebral gas embolism (arterial) with special reference to iatrogenic accidents. HBO Rev 1980; 1: 161-84.

10. Mansour A, AbdelRaouf S, Qandeel M, *et al*. Acute coronary artery air embolism following CT-guided lung biopsy. Cardiovasc Intervent Radiol 2005; 28: 131-4.

成功以高壓氧治療電腦斷層引導肺穿刺切片併發之氣栓塞

陳威廷　陳炯睿

電腦斷層引導之肺切片是一項被廣泛接受且經常實施之診斷工具，然而其亦有存在著不同之併發症，例如氣胸、咳血及肺出血。輕度自行復原之氣胸及咳血為最常見之併發症，氣栓塞是一種具有致命危險但極罕見之併發症。我們報告一位因接受電腦斷層引導之切片併發空氣栓塞存在於上升主動脈，並成功以高壓氧治療移除其空氣栓塞，沒有遺留心臟或腦部之併發症之案例。*(胸腔醫學 **2018; 33: 89-94**)*

關鍵詞：電腦斷層引導之肺切片，空氣栓塞

國立成功大學醫學院及醫院　內科學科
索取抽印本請聯絡：陳炯睿醫師，國立成功大學醫學院及醫院　內科學科，台南市勝利路 138 號